Journal of Visualized Experiments

The Fabrication and Operation of a Continuous Flow, Micro-Electroporation System with Permeabilization Detection.

--Manuscript Draft--

Article Type:	Methods Article - JoVE Produced Video
Manuscript Number:	JoVE63103R2
Full Title:	The Fabrication and Operation of a Continuous Flow, Micro-Electroporation System with Permeabilization Detection.
Corresponding Author:	Jeffrey Zahn Rutgers University: Rutgers The State University of New Jersey Piscataway, New Jersey UNITED STATES
Corresponding Author's Institution:	Rutgers University: Rutgers The State University of New Jersey
Corresponding Author E-Mail:	jdzahn@soe.rutgers.edu
Order of Authors:	Joseph J. Sherba
	Maria Atzampou
	Hao Lin
	Jerry W. Shan
	David I. Shreiber
	Jeffrey Zahn
Additional Information:	
Question	**Response**
Please specify the section of the submitted manuscript.	Bioengineering
Please indicate whether this article will be Standard Access or Open Access.	Standard Access ($1400)
Please indicate the **city, state/province, and country** where this article will be **filmed**. Please do not use abbreviations.	Piscataway, New Jersey, United States
Please confirm that you have read and agree to the terms and conditions of the author license agreement that applies below:	I agree to the Author License Agreement
Please confirm that you have read and agree to the terms and conditions of the video release that applies below:	I agree to the Video Release
Please provide any comments to the journal here.	

TITLE:

The Fabrication and Operation of a Continuous Flow, Micro-Electroporation System with Permeabilization Detection.

AUTHORS AND AFFILIATIONS:

Joseph J. Sherba[1], Maria Atzampou[1], Hao Lin[2], Jerry W. Shan[2], David I. Shreiber[1], Jeffrey D. Zahn[1]

[1]The Department of Biomedical Engineering, Rutgers, The State University of New Jersey, Piscataway, NJ, USA

[2]The Department of Mechanical and Aerospace Engineering, Rutgers, The State University of New Jersey, Piscataway, NJ, USA

Email addresses of co-authors:

Joseph J. Sherba (jjs5476@gmail.com)
Maria Atzampou (m.atzampou@rutgers.edu)
Hao Lin (hlin@soe.rutgers.edu)
Jerry W. Shan (jshan@soe.rutgers.edu)
David I. Shreiber (shreiber@soe.rutgers.edu)
Jeffrey D. Zahn (jdzahn@soe.rutgers.edu)

Corresponding author:

Jeffrey D. Zahn (jdzahn@soe.rutgers.edu)

KEYWORDS:

electroporation, microfluidics, lab-on-a-chip, biosensor, transfection, electro-transfection, intracellular delivery

SUMMARY:

This protocol describes the microfabrication techniques required to build a lab-on-a-chip, microfluidic electroporation device. The experimental setup performs controlled, single-cell-level transfections in a continuous flow and can be extended to higher throughputs with population-based control. An analysis is provided showcasing the ability to electrically monitor the degree of cell membrane permeabilization in real-time.

ABSTRACT:

Current therapeutic innovations, such as CAR-T cell therapy, are heavily reliant on viral-mediated gene delivery. Although efficient, this technique is accompanied by high manufacturing costs, which has brought about an interest in using alternative methods for gene delivery. Electroporation is an electro-physical, non-viral approach for the intracellular delivery of genes and other exogenous materials. Upon the application of an electric field, the cell membrane temporarily allows molecular delivery into the cell. Typically, electroporation is performed on the macroscale to process large numbers of cells. However, this approach requires extensive empirical protocol development, which is costly when working with primary and difficult-to-transfect cell types. Lengthy protocol development, coupled with the requirement of large

voltages to achieve sufficient electric-field strengths to permeabilize the cells, has led to the development of micro-scale electroporation devices. These micro-electroporation devices are manufactured using common microfabrication techniques and allow for greater experimental control with the potential to maintain high throughput capabilities. This work builds off a microfluidic-electroporation technology capable of detecting the level of cell membrane permeabilization at a single-cell level under continuous flow. However, this technology was limited to 4 cells processed per second, and thus a new approach for increasing the system throughput is proposed and presented here. This new technique, denoted as cell-population-based feedback control, considers the cell permeabilization response to a variety of electroporation pulsing conditions and determines the best-suited electroporation pulse conditions for the cell type under test. A higher-throughput mode is then used, where this 'optimal' pulse is applied to the cell suspension in transit. The steps for fabricating the device, setting up and running the microfluidic experiments, and analyzing the results are presented in detail. Finally, this micro-electroporation technology is demonstrated by delivering a DNA plasmid encoding for green fluorescent protein (GFP) into HEK293 cells.

INTRODUCTION:

Current therapeutic innovations in biomedical research, such as CAR-T (Chimeric Antigen Receptor Engineered T cell) cell therapy and genetic editing using CRISPR (clustered regularly interspaced short palindromic repeat DNA sequences)/Cas9, heavily rely on the ability to deliver exogenous material both successfully and efficiently into the intracellular space[1]. In CAR-T therapy, the gold standard to perform the gene delivery step in cell therapy manufacturing is using viral vectors[2]. Though viral-mediated gene delivery is an efficient delivery modality, it also has several drawbacks. These include manufacturing costs, cytotoxicity, immunogenicity, mutagenesis/tumorigenesis potential, and size limitations on the gene(s) to be delivered[3]. These limitations have led to the research and development of alternative, non-viral delivery technologies.

Electroporation, an alternative to viral-mediated gene delivery, relies on the application of an optimal electrical pulse waveform to perform DNA, RNA, and protein transfections of cells. Following the application of an external electric field, the cell membrane is briefly compromised, making the cell susceptible to the intracellular delivery of otherwise impermeable exogenous materials[4]. Compared to viral-mediated delivery, electroporation is advantageous as it is generally safe, easy to operate, and has low operating costs. Electroporation can deliver both small and large molecular cargo and can be efficient in transfecting cells regardless of lineage[5]. To achieve desirable outcomes following electroporation, i.e., good viability and good electro-transfection efficiency, a variety of experimental parameters need to be co-optimized. These include cell type[6], cell density, molecule concentration[7], electroporation buffer properties (e.g., molecular composition, conductivity, and osmolarity)[8], electrode size/geometry[9], and electrical pulse waveform (shape, polarity, number of pulses)[10] (refer to **Figure 1** for an illustration). Although each of these parameters can have a significant effect on the outcomes of electroporation experiments, pulse waveform has been especially studied in great detail, as the electrical energy of the applied pulse(s) is the root of the intrinsic trade-off between the resulting cell viability and electro-transfection efficiency[8].

Typically, electroporation experiments are performed on the macro-scale, where cells are suspended in 100s of microliters of buffer between a set of large, parallel-plate electrodes within an electroporation cuvette. The electrodes are commonly manufactured out of aluminum with an electrode distance of 1–4 mm. Once the cells are manually loaded via pipette, the cuvette is electrically connected to a bulky, electrical pulse generator where the user can set and apply the pulse waveform parameters to electroporate the cell suspension. Although macro-scale or bulk electroporation can process cell densities >10^6 cells/mL, this feature can be wasteful when optimizing the electrical pulse waveform settings. This is particularly of concern when electroporating primary cell types where the cell population numbers can be limited. Additionally, due to the large distance between the electrodes, the pulse generator must be able to supply large voltages to achieve electric field strengths >1kV/cm[11]. These high voltages cause resistive power dissipation through the electrolyte buffer resulting in Joule heating, which can be detrimental to the resulting cell viability[12]. Lastly, performing electroporation on a dense suspension of cells will consistently be burdened with an innate variability in the resulting electro-transfection efficiency and cell viability. Each cell in suspension could experience a different electric field strength due to the surrounding cells. Depending on whether the experienced electric field strength is either increased or decreased, the resulting cell viability or electro-transfection efficiency may each be negatively impacted[11]. These downsides to macro-scale electroporation have led to the pursuit and development of alternative technologies that operate on the micro-scale and allow for better control at the single-cell level.

The field of BioMEMS, or biomedical micro-electro-mechanical systems, stems from the technological advancements made in the microelectronics industry. Specifically, utilizing microfabrication processes to develop micro-devices for the advancement of biomedical research. These advancements include the development of micro-electrode arrays for *in vivo* electrical monitoring[13], capacitive micro-electrodes for in situ electroporation[14], miniaturized organ-on-a-chip devices[15], microfluidic point-of-care diagnostics[16], biosensors[17], and drug delivery systems[18], including nano- and micro-electroporation devices[19–21]. Due to the ability to design and manufacture devices at the same size scale as biological cells, nano- and micro-electroporation technologies are advantageous when compared to their macro-scale counterpart[22,23]. These electroporation devices eliminate the requirement of high voltage pulse applications, as electrode sets with spacings of 10s to 100s of micrometers are typically integrated. This feature drastically reduces the current through the electrolyte, which in turn reduces the accumulation of toxic electrolysis products and the effects of Joule heating in these systems. The micro-scale channels also ensure that a much more uniform electric field is reliably applied to the cells during pulse application, resulting in more consistent outcomes[24]. In addition, it is also commonplace for micro-electroporation devices to be integrated into a microfluidic platform which lends itself for future integration into a fully automated technology, a highly desirable capability in cell therapy manufacturing[25]. Lastly, micro-scale electroporation allows for the electrical interrogation of electroporation events. For example, the degree of cell membrane permeabilization can be monitored in real-time at a single cell level[26,27]. The purpose of this method is to describe the microfabrication, system operation, and analysis of a microfluidic, single-cell micro-electroporation device capable of measuring the degree of cell membrane

permeabilization for optimizing electroporation protocols, yet increasing throughput over the previous state-of-the-art.

Performing single-cell level electroporation is no longer a novel technique, as it was first demonstrated by Rubinsky et al. in 2001 with the development of a static cell electroporation technology[28]. Their micro-device was innovative as they were the first to demonstrate the ability to electrically monitor the event of electroporation. This has further led to the development of static, single-cell electroporation technologies capable of electrically detecting the degree of cell membrane permeabilization in a parallelized manner to increase the throughputs of the devices. However, even with parallelization and batch processing, these devices severely lack the total number of cells they can process per unit time[29,30]. This limitation has led to the development of flow-through devices capable of performing single-cell level micro-electroporation at much greater throughputs[31]. This device transition, from static to flow-through environment, limits the capability of electrically monitoring the degree of cell membrane permeabilization following the application of the electroporation pulse. The method described in this work bridges the gap between these two technologies, a micro-electroporation technology capable of electrically detecting, pulsing, and monitoring the degree of cell membrane permeabilization of individual cells, in a continuous-flow, serial fashion.

This technology was recently described in Zheng et al. In that work, the capabilities of this technology were introduced with the completion of a parametric study, where both the amplitude and duration of the electroporation pulse were varied, and the ensuing electrical signal, indicative of cell membrane permeabilization, was explored[32]. The results showed that an increase in the intensity of the electroporation pulse (i.e., increase in applied electric field or increase in pulse duration) caused an increase in the measured cell membrane permeabilization. To further validate the system, a common fluorescent indicator of successful electroporation, propidium iodide[33], was added to the cell suspension, and a fluorescence image was captured immediately following the application of the electrical pulse. The optical signal, i.e., the fluorescence intensity of propidium iodide inside the cell, was strongly correlated with the electrical measurement of the degree of cell membrane permeabilization, verifying the reliability of this electrical measurement. However, this work only considered the delivery of the small molecule propidium iodide, which has little to no translatable significance.

In this work, a new application of this technology is introduced to improve upon the throughput of the system while delivering a biologically active plasmid DNA (pDNA) vector and assessing the electro-transfection efficiency of cells replated and cultured following electroporation. Though the previous work outperforms existing micro-electroporation technologies that are capable of electrically measuring the event of electroporation, the current state of the device still requires long cell transit times between the electrode set (~250 ms) to perform the cell detection, pulse application, and the cell membrane permeabilization measurement. With a single channel, this limits the throughput to 4 cells/s. To combat this limitation, a new concept of cell-population-based feedback-controlled electroporation is introduced to perform pDNA electro-transfection. By using a hypo-physiologic conductivity electroporation buffer, this system allows for the electrical interrogation of single cells across a multitude of electroporation pulse applications.

Based on the electrical response, an 'optimal' electroporation pulse is then determined. A 'high-throughput' mode is then implemented where the cell membrane permeabilization determination is nullified, the flow rate is increased, and the electroporation pulse duty cycle is matched to the cell transit time to ensure one pulse per cell in transit between the electrodes. This work will provide extensive details into the microfabrication steps for the manufacturing of the micro-device, the material/equipment and their setup required to perform the experimentation, and the operation/analysis of the device and its electro-transfection efficiency (eTE).

[Place **Figure 1** here]

PROTOCOL:

NOTE: Users should review all MSDS for the materials and supplies used in this protocol. Appropriate PPE should be worn at each step and sterile technique used during experimentation. Sections 1–7 discuss the device fabrication.

1. Device fabrication- Mask design

NOTE: Refer to **Figure 2** for an illustration of the microfabrication process. The microfabrication steps are to be carried out in a cleanroom environment. Additional PPE is necessary (hair net, facial hair net, mask, cleanroom suit, shoe covers).

1.1. Install a CAD software of choice, design a 2-Dimensional 'mask' of both the microfluidic channel and electrodes and save the design in desired file format (i.e., .dxf, .dwg).

NOTE: Refer to **Supplementary Figure 1** for an example of a 2-Dimensional mask schematic.

1.2. Send to a supplier of choice to be printed. Ensure the dimensions of the designs are within the resolution capabilities of the supplier.

2. Device fabrication- Photolithography

NOTE: The provided microfabrication recipes are adopted from the photoresists' manufacturer's recommendations and should only be used as a starting point[34]. Exact values for baking times, exposure times, etc., need to be optimized for each fabrication protocol. It is recommended to use wafer tweezers for handling both silicon wafers and glass slides.

2.1. Microfluidic channel fabrication

2.1.1. Silicon wafer and soda-lime glass slide cleaning: Follow steps 2.1.2–2.1.3 to perform silicon wafer and 1" × 3" soda-lime glass slide cleaning (both referred to as 'substrate').

2.1.2. Submerge the substrates in an acetone bath, an isopropanol (IPA) bath and a deionized

water bath for 10 min each. Perform this 3-step wash serially at room temperature.

2.1.3. Remove and dry the surface using a pressurized nitrogen or filtered air gas source. Place the substrates into a 150 °C oven for a minimum of 30 min to allow evaporation of the remaining moisture.

2.1.4. SU-8 photolithography on silicon wafer: Perform photolithography on the silicon wafer following steps 2.1.5–2.1.14.

NOTE: To achieve a microfluidic channel height of 20 µm, SU-8 2000 series negative photoresist was used. Exact spin rates will vary depending on the formulation of SU-8 (i.e., 2010, 2015, etc.); however, the following conditions are for the SU-8 2010 formulation[35].

2.1.5. Remove the silicon wafer from the 150 °C oven and allow it to cool to room temperature (RT).

2.1.6. Secure the wafer to the chuck of the wafer spin coater using the spin coater's vacuum system. Program the spinner. Step 1 – 500 rpm for 10 s at an acceleration of 100 rpm/s, Step 2 – 1000 rpm for 30 s at an acceleration of 300 rpm/s.

2.1.7. Dispense 4 mL of SU-8 2010 photoresist onto the center of the silicon wafer. Run the program. Once the system comes to a halt, turn off the vacuum.

2.1.8. Using tweezers, transfer the SU-8 coated silicon wafer on a hot plate at 95 °C for 4–5 min for soft bake. Then remove the wafer from the hot plate and allow it to cool to RT.

NOTE: Follow the proper start up procedure for the lab-specific photolithographic mask aligner.

2.1.9. Secure the photomask with the 2D microfluidic channel designs onto the mask holder. Insert the silicon wafer, with the SU-8 coating facing upwards, onto the wafer chuck.

2.1.10. Set the exposure settings for 150 mJ/cm^2 and run the machine.

CAUTION: Do not look directly at the UV light source to avoid potential eye damage.

2.1.11. Place the SU-8 coated silicon wafer on a hot plate at 95 °C for 4–5 min for post-exposure bake.

2.1.12. Submerge the silicon wafer in the SU-8 developer solution (see **Table of Materials**) for 3–4 min. Apply gentle agitation. Remove the wafer from the solution and rinse the surface with IPA.

2.1.13. Dry the surface using a pressurized nitrogen or filtered air gas source. Inspect the features under a microscope using a UV filter and ensure no obvious defects in the microfluidic channels.

2.1.14. Place the silicon wafer into a 150 °C oven for a minimum of 30 min for a hard bake.

2.1.15. Allow to cool down to RT and use stylus profilometry to measure the exact height and slope of the channel sidewalls.

2.2. Photolithography on Glass Slides

NOTE: Hexamethyldisilazane (HMDS) is used as an adhesion promoter for the S1818 positive photoresist[36].

2.2.1. Remove the glass slide from the 150 °C oven and allow it to cool to RT.

2.2.2. Secure the glass slide to the chuck of the spinner using vacuum and program the spinner. Step 1 – 500 rpm for 10 s at an acceleration of 100 rpm/s. Step 2 – 3000 rpm for 30 sat an acceleration of 300 rpm/s.

2.2.3. Dispense 3—4 droplets of HMDS across the surface of the glass slide. Run the program.

NOTE: To achieve a surface coating of ~3 µm, S1800 positive photoresist series should be used. Exact spin rates will vary depending on the formulation; the recommendations below are for the S1818 formulation[34].

2.2.4. Dispense 1 mL of photoresist onto the surface of the glass slide. Ensure enough to cover the surface area.

2.2.5. Run the program. Once the system comes to a halt, turn off the vacuum, and remove the glass slide.

2.2.6. Place the S1818 coated glass slide on a hot plate at 120 °C for 4 min for a soft bake. Remove and allow to come to RT.

2.2.7. Secure the photomask with the 2D electrode designs onto the mask holder.

2.2.8. Insert and align the glass wafer, with the S1818 coating facing upwards, onto the wafer chuck. Set the exposure settings for 250 mJ/cm^2 and run the machine.

NOTE: Different contact aligner models may be more or less accommodating to non-circular, varying thickness substrates.

2.2.9. Submerge the glass slide in MF-319 developer solution for 2 min. Apply gentle agitation. Rinse the surface of the wafer with IPA.

2.2.10. Dry the surface using a pressurized nitrogen or filtered air gas source and observe the features under a microscope using a UV filter. Make sure there are no obvious defects in the

lithographic patterns.

2.2.11. Place glass slide into the 150 °C oven, ensuring substrate surface of interest is facing up, for a minimum of 30 min for a hard bake. Remove from the oven and keep protected from light.

3. Device fabrication: Hydrofluoric acid (HF) etch

CAUTION: This step involves the handling and disposal of hydrofluoric acid (HF), which can cause deep, painful chemical burns. Additional PPE should be used to protect the handler (face shield, elbow-length chemically resistant gloves, chemically resistant apron with sleeves). Calcium gluconate acid neutralizer and skin gel should be kept in proximity of the lab bench. This step should not be performed alone. HF should never be stored in or dispensed into glass containers as the container will be etched by the acid.

NOTE: The HF uniformly etches the exposed glass (i.e., the electrode design) to form a recess in the glass, allowing for better edge resolution of the electrode pattern after metal deposition (section 4).

3.1. Submerge the glass slide in 10:1 buffered HF solution for 1 min in a polytetrafluoroethylene container. Transfer and wash the glass slides in deionized water. Repeat the wash step 3 times.

3.2. Dry the surface using a pressurized nitrogen or filtered air gas source. Place glass substrates in a 65 °C oven overnight to remove any remaining moisture. Cover the substrates from light.

4. Device fabrication: Physical vapor deposition

NOTE: This step involves the metal deposition onto the glass slide substrates to define the electrode patterns. Commonly used metal electrodes are chromium/gold and titanium/platinum. Gold and platinum do not adhere to the glass substrate, so a seed adhesion layer of chromium or titanium, respectively, is required to promote adhesion[37].

4.1. Follow the cleanroom-specific protocol to operate the in-house PVD system. This work uses a DC sputtering system and sputter with 100 SCCM Argon gas at a pressure of ~8 mTorr and 200 W power.

4.2. Sputter titanium for 8 min at a rate of ~100 Å/min. Sputter platinum for 10 min at a rate of ~200 Å/min. Remove the substrates from the PVD chamber.

5. Device fabrication: Photoresist lift-off

NOTE: This step involves dissolving the photoresist layer in an acetone bath, leaving the adhered platinum electrodes patterned on the glass slides.

5.1. Submerge the metal-coated glass slides in an acetone bath for ~10 min.

5.2. Sonicate the bath to introduce agitation to break up the unadhered metal film. Use an acetone-soaked wipe to remove any residues if necessary.

5.3. Once all photoresist/metal is removed, wash the electrode patterns with deionized water, and place them in a 65 °C oven overnight to remove any remaining surface moisture.

5.4. Use stylus profilometry to measure the profile of the patterned electrodes.

6. Device fabrication: Soft lithography

NOTE: This step involves replica molding the microfluidic channel onto the SU-8 master relief structure using an elastomer, polydimethylsiloxane (PDMS).

6.1. Silicon wafer silanization

NOTE: This is an optional step; however, it will increase the lifetime of the SU-8 relief structure that was fabricated in subsection 2.1.

6.1.1. Secure the wafer to the bottom of a Petri dish and place the Petri dish into a desiccator.

6.1.2. Surround the perimeter of the silicon wafer with approximately 50 µL of Trichloro(1H,1H,2H,2H-perfluorooctyl) silane. Connect vacuum (vacuum pump or house vacuum line) and run for 20 min.

6.2. PDMS replica molding

6.2.1. In a disposable container (e.g., weigh boat, plastic cup), mix PDMS elastomer base to hardener at a 10:1 weight ratio on top of an electronic balance. Pour the PDMS solution over the silicon wafer and place the mixture under a vacuum to remove all air bubbles.

6.2.2. Cure at 65 °C for a minimum of 4 h allowing the PDMS to solidify. Using the tip of a razor blade, cut out the molded PDMS and peel from the silicon wafer.

6.2.3. Using a sharpened biopsy punch, remove PDMS from the inlet/outlets of the device. For this device, 0.75 mm and 3 mm biopsy punches were used for the inlets and the outlets, respectively.

NOTE: The biopsy punch used should have a slightly smaller diameter than the outer diameter of the interconnecting tubing to ensure a tight seal of tubing in the reservoirs.

6.3. Sonication cleaning of PDMS

6.3.1. Submerge the PDMS devices in IPA and place them into a sonicator for 30–45 min to remove any PDMS debris from the inlet/outlets. PDMS may swell in the IPA solution.

6.3.2. Rinse with deionized water and place in a 65 °C oven overnight to allow the PDMS to de-swell back to the normal size.

NOTE: Any leftover debris can clog the device during experimentation. Large pieces of debris can be removed from the PDMS surface using a piece of scotch tape prior to sonication.

7. Device fabrication: PDMS bonding/wire attachment

NOTE: This step involves treating the surface of the PDMS and glass substrate with an oxygen plasma to form an irreversible bond between the PDMS and glass[38]. The recipe provided may need to be adapted to the exact system used in the laboratory.

7.1. Cut the devices to size and ensure the surface of the PDMS device is clean. If not reclean, follow the steps in subsection 6.3.

7.2. Program the plasma generator. Set **Power** to 70 W, **Time** to 35 s, **Pressure** to 325 mTorr, **Flow Rate** of oxygen gas to 60 SCCM. Place PDMS and electrode glass slide into the system with the features facing up and run the program.

7.3. Remove the devices and quickly align channel features to the electrodes using a stereoscope. Firmly apply pressure from the center of the PDMS towards the sides to remove any unwanted air bubbles at the bonding interface.

7.4. Place on a hot place at 95 °C for at least 2 min to finalize the bonding procedure and let the device cool down at RT.

7.5. Cut 2 pieces of 22-G solid wire at ~6” lengths and strip the insulator from both ends.

7.6. Bond the wires to electrode pads using silver conductive epoxy. Place completed devices in a 65 °C oven overnight.

[Place **Figure 2** Here]

8. Cell culture and harvest

NOTE: Standard cell culture and sterile handling procedures should be utilized. Follow cell-type-specific protocol for cell culture.

8.1. Cell culture

8.1.1. Cell passage: Culture and passage the cells following steps 8.1.2–8.1.5.

8.1.2. Culture HEK293 cells in complete DMEM solution (88% DMEM, 10% heat-inactivated fetal bovine serum, 1% L-glutamine, 1% penicillin-streptomycin) in a T25 flask in an incubator at 37 °C, 95% O2, 5% CO2. Passage cells on schedule when reaching ~80% confluency.

8.1.3. Aspirate the media using either a pipette or vacuum system and incubate the cells in 0.25% trypsin-EDTA (2 mL—T25 flask) for 2 min at 37 °C. Neutralize trypsin with twice the volume of culture media.

8.1.4. Transfer the cell suspension into a 15 mL conical tube and centrifuge HEK293 cells at 770 x *g* for 2 min. Aspirate the supernatant using either a pipette or vacuum system

8.1.5. Resuspend HEK293 cells in 1 mL of pre-warmed DMEM.

8.1.6. Cell plating: Plate the cells following steps 8.1.7–8.1.8

8.1.7. Plate the cells at a 10:1 to 20:1 dilution in a T25 flask (5 mL of DMEM) to continue the culture.

8.1.8. Plate the cells at a 5:1 to 20:1 dilution in a 6-well plate (2 mL of DMEM per well) to be harvested for electroporation experiments.

NOTE: HEK293 cells plated 24 h prior to electroporation experiments to achieve ~70% confluency at cell harvest (subsection 8.3). An inconsistent harvest schedule can lead to variability in electroporation results.

8.2. Electroporation buffer

8.2.1. Prepare electroporation buffer

NOTE: Refer to Sherba et al. for specifics on the electroporation buffer preparation[8]. The buffer composition was 285 mM Sucrose, 0.7 mM $MgCl_2$, 1 mM KCl, 10 mM HEPES, 3 mM NaOH (pH: 7.4; osmolality: 310 mOsm, conductivity: 500 µS/cm). Electroporation buffer should be formulated in a sterile fashion and stored at 4 °C for a shelf life of ~1 month. Electroporation buffer formulation should be optimized on a per cell type basis.

8.3. Cell harvest and pDNA addition

8.3.1. Follow the same steps as cell passage (8.1.2–8.1.4).

8.3.2. Wash the cells in sterile 1x PBS, transfer-cell suspension into a 15 mL conical tube, and centrifuge cells at 770 x *g* for 2 min.

8.3.3. Wash HEK293 cell pellet in the electroporation buffer and centrifuge at 770 x *g* for 2 min. Resuspend the cells in the electroporation buffer at ~5 million cells/mL.

NOTE: Cell density should be optimized per cell type.

8.3.4. Add pDNA encoding for green fluorescent protein (GFP) to a final concentration of 20 µg/mL. Gently mix the pDNA/cell suspension and transfer the suspension into a 1 cc syringe for experimentation.

9. Hardware/experimental setup

NOTE: Prior to harvesting cells for experimentation, ensure the experimental setup is completed to minimize the amount of time the cells are suspended in the electroporation buffer. Turn on electronics 20–30 min prior to experiments to warm up. Refer to **Figure 3** for a schematic of the experimental setup for the operation of the single-cell detection module.

NOTE: A custom-built PA90 Op-Amp circuit was developed to accommodate both the sensitivity required for single-cell level detection using the lock-in amplifier and the high voltages required to apply sufficiently strong electroporation pulses. Refer to PA90 datasheet for specifications on recommended circuitry[39].

9.1. Initialize the Lock-in Amplifier with Current Pre-Amplifier settings and set via the algorithm. Refer to Zheng et al. for specifics on the lock-in settings[32].

9.2. Power supplies, function generator, and amplifier

9.2.1. Power Supply 1: Set to -15 V to power the negative end of the circuit.

9.2.2. Power Supply 2 (Function Generator): Set to output DC signal and set the amplitude to 2 V. Connect to 50x amplifier input.

9.2.3. Program Electroporation Pulse Generator for the square wave: Set the desired pulse width (duty cycle) and desired pulse amplitude (Volts).

9.2.4. Set output to trigger mode (1 pulse). Connect the output to the input of the 50x amplifier.

NOTE: Remember the 50x gain when programming the pulse amplitude. I.e., to achieve an electric field strength of 1 kV/cm, a total of 30 V is required, 30 V/300 µm (distance between electrodes), therefore the function generator output should be set to 30/50, or 600 mV.

9.2.5. Verify the outputs of the 50x Amplifier using an oscilloscope. Output 1—100 V from Power Supply 2 (9.2.2). Output 2—Variable amplitude for the electroporation pulse (9.2.4).

9.2.6. Connect a 10x probe to an oscilloscope channel and to the completed micro-device

(device under test, DUT) in step 7.6 where the electroporation pulse is going to be applied. Monitor the system during experimentation to ensure pulses are being applied.

9.2.7. Ensure lock-in USB is connected and registered. Double-check all lock-in settings in the algorithm code (most importantly, lock-in output frequency).

9.3. Microscope/CCD camera

9.3.1. Place the micro-device onto the stage of the microscope via a slide holder. Turn on the CCD camera and bring the microfluidic channel into focus. Use a 4x or 10x objective.

[Place **Figure 3** Here]

10. Experimental operation

10.1. Microfluidic channel priming

10.1.1. Remove all air bubbles from the cell-loaded syringe. Attach a 30 G needle to the cell-loaded syringe.

10.1.2. Using tweezers, slide tygon tubing down the length of the needle. Pre-fill the outlet reservoir with recovery media (same as step 8.1.2 without the antibiotics), ~40–50 µL.

10.1.3. Using the thumb, gently apply pressure to the plunger such that the fluid slowly reaches the end of the tubing line.

10.1.4. Secure the syringe to the syringe pump. Turn the syringe pump on and ensure it is set to forward perfusion.

10.1.5. Program the pump for the proper diameter of the syringe to ensure flow rates are accurate. Refer to pump manual for specifics on syringe diameters.

NOTE: To prevent cells from settling in the syringe, secure the syringe pump on a clamp stand such that it can operate in a vertical position with the syringe end facing downwards.

10.1.6. Set syringe pump flow rate, ~10–20 µL/min, and allow the pump to run until the fluid reaches the end of the tubing line. Secure tubing to the microfluidic device.

10.1.7. Lower the syringe pump flow rate, ~5–10 µL/min, and allow the pump to run until all air is expelled from the microfluidic device and cells are traversing to the device outlet.

10.1.8. Remove the cells from the outlet via pipette aspiration. Re-fill the outlet reservoir with recovery media (same as step 8.1.2 without the antibiotics), ~40–50 µL.

10.2. Single-cell electroporation—cell membrane permeabilization mapping

NOTE: Refer to **Figure 4** and **Figure 5** for a better understanding of the electrical data indicative of cell membrane permeabilization and the cell membrane permeabilization mapping, respectively.

10.2.1. Set the syringe pump flow rate to ~0.1–0.3 µL/min to ensure a flow of single cells through the electrode set. The cell transit time between the electrodes should be ~250 ms.

10.2.2. Start the computer program by clicking on **Run**. Ensure the system is saving the electrical data.

10.2.3. Ensure the system is reliably detecting cells to trigger the computer-controlled pulse applications. Adjust **Detection Threshold** accordingly.

10.2.4. Set the pulse parameters for the initial, lowest electrical energy electroporation pulse. Refer to **Table 1** for electroporation pulsing parameters in this study.

10.2.5. Turn on the Output channel for the electroporation pulse generator (step 9.2.3.).

10.2.6. Follow a pre-determined number of cell detection/pulse applications (n =100). At the end of each tested condition, aspirate cells from the microdevice outlet and replenish the outlet with recovery media.

10.2.7. Iterate to the next electroporation pulse condition. Repeat until all electroporation pulse conditions are tested.

10.2.8. Determine the degree of cell membrane permeabilization for each pulse application tested. (Post-process validation is described in subsection 11.1). Generate the cell membrane permeabilization map (**Figure 5**).

10.2.9. Determine the electroporation pulse parameters for high-throughput, population-based feedback.

10.2.10. Turn off the syringe pump, remove cells from the outlet reservoir, and replenish the outlet with recovery media.

10.3. Population-based feedback-controlled electroporation—high throughput

NOTE: Refer to **Figure 6** for a schematic illustrating the population-based feedback process.

10.3.1. Set the syringe pump flow rate to ~1–3 µL/min to ensure a flow of single cells through the electrode set. The cell transit time between the electrodes should be ~25 ms.

10.3.2. Set the pulse amplitude to the 'optimized' condition (10.2.9), turn off trigger mode, and set the pulse width to match the cell transit time.

10.3.3. Set the duty cycle such that pulse ON time matches the 'optimized' condition. Refer to **Table 1**.

10.3.4. Set the Output channel function generator to **ON**, turn on the syringe pump, and allow the system to run until the desired number of cells have been electroporated.

10.3.5. When done, turn off both the syringe pump and the function generator.

10.3.6. Transfer the cells from the outlet reservoir into the appropriately sized cell culture flask/plate filled with pre-warmed recovery media and transfer culture flask/plate into the incubator.

11. Analysis

11.1. Single-cell level membrane permeabilization detection

NOTE: To ensure the 'optimal' pulse was used during the high throughput module, a post-experiment analysis should be performed to verify the electrical data exported from subsection 10.2. Please refer to **Figure 4** for a graphical representation of the electrical signal representative of membrane permeabilization due to electroporation.

11.1.1. Load data into an analysis software (MATLAB, Python, etc.). Generate a plot of Current versus Time for each pulsing condition.

11.1.2. Manually determine the degree of cell membrane permeabilization ($\Delta I_P/\Delta I_C$). Refer to **Figure 4**. Generate the Cell Membrane Permeabilization Map (ΔI_P / ΔI_C versus Electrical Energy, **Figure 5**) over all tested pulse conditions. Verify 'optimal' pulsing condition.

11.2. electro-Transfection Efficiency (eTE)

11.2.1. Following the 24-h incubation period, remove the electroporated cells from the incubator.

11.2.2. Perform a live cell stain. Dilute DRAQ5 1:1000 to a final concentration of 5 µM in the cell culture vessel. Gently mix the cells/staining solution and incubate at 37 °C for 5–30 min.

NOTE: A different stain can be implemented in this step. Ensure that the fluorescent properties do not overlap with the fluorescent marker indicating successful electro-transfection (i.e., GFP is in the green wavelength and DRAQ5 is the far-red).

11.2.3. Turn on an epifluorescent microscope, lamp, and cameras (see **Table of Materials**).

11.2.4. Remove the cells from the incubator and bring them into focus on the microscope.

11.2.5. Capture a phase-contrast image (brightfield) of the selected field.

11.2.6. Capture epifluorescent images of the same field using FITC (GFP) and Far-Red (DRAQ5) filters. Analyze the image sets manually or via an algorithm.

NOTE: Refer to **Figure 7** for representative images.

11.2.7. Count the total number of GFP-positive cells in all the images. Count the total number of DRAQ5 stained cells in all the images. Calculate eTE (ratio of GFP positive cells to DRAQ5 stained cells).

REPRESENTATIVE RESULTS:

Figure 4 highlights the operating principles behind the single-cell-level membrane permeabilization detection for a single pulse amplitude. Following the initiation of the electroporation experiment, the cell detection algorithm determines an optimal threshold for cell detection via a point-by-point, slope-based detection method. The system then continuously monitors (1) for a significant negative change in the measured electrical current, which is indicative of the entry of a cell. This is due to the insulative nature of the biological cell membrane, such that when the cell traverses through the electrode set, there is an instantaneous increase in impedance, resulting in a sharp, decrease in the measured current, allowing for consistent cell detection (2), which ultimately triggers the switch to the computer-controlled pulse application (4). The insulated cell displaces a volume of electrolyte between the electrodes, resulting in a drop in current that is proportional to the size of the cell. This change in current is denoted as ΔI_C (3). Immediately following ΔI_C calculation, the pre-determined, electrical pulse is administered (4) to the cell in transit. This instantaneous influx of energy introduces a brief sensing artifact into the system (grey box). Upon re-locking onto the signal, i.e., switching back to cell monitoring, (5) it is evident that the electroporation pulse permeabilized the cell membrane as the magnitude of current change due to the cell's presence between the electrode set drops upon exit (6). The difference in the two drops in current due to the cell's impedance magnitude pre/post electroporation pulse application is termed the permeabilization current and is denoted as ΔI_P. Once the cell exits the volume between the electrodes, the baseline stabilizes, and the system returns to cell detection mode (1). After a pre-determined number of cells are electroporated, the next highest energy electroporation pulse is tested (Refer to **Table 1** for pulse settings). For each electroporation pulse tested, an average 'degree of membrane permeabilization' is determined. This value is calculated as $\Delta I_P/\Delta I_C$. Once each pre-determined electroporation pulse is tested, the $\Delta I_P/\Delta I_C$ is plotted against the applied electrical energy density (σ x E^2 x t), where σ is the solution conductivity (S/cm), E is the electric field strength (kV/cm), and t is the pulse duration (ms). Refer to **Figure 5** for the cell membrane permeabilization map for HEK293 cells used in this example.

[Place **Table 1** Here]

[Place **Figure 4** Here]

A distinct correlation is observed between the applied electrical energy and the degree of cell membrane permeabilization (**Figure 5**), with the existence of a transition region where a substantial increase in the degree of cell membrane permeabilization occurs. To that end, a pulse with electrical energy that surpasses this transition region is selected for the high-throughput phase of the micro-electroporation process (**Figure 6**). In this experiment, the 1.8 kV/cm: 670 µs pulse was determined as 'optimal'. As was described in detail in subsection 10.3 of the protocol, the system flow rate is increased, and the function generator set to continuously output a pulse with a set pulse and duty cycle (refer to **Table 1** for pulse settings for 1.5 µL/min and 3.0 µL/min flow rates) to ensure 1 pulse is applied to each cell in transit. In this study, the flow rate was increased by 5x, thus the pulse width was set to 50 ms (matching the cell transit time) at a duty cycle (d.c.) of 2.7%.

[Place **Figure 5** Here]
[Place **Figure 6** Here]

Following 24 h of post-electroporation recovery, the cells were imaged to determine the electro-transfection efficiency (eTE). As described in subsection 11.2 of the protocol, the eTE was determined as the total number of cells expressing GFP normalized to the total number of cells stained with DRAQ5. The eTE for the 1.8 kV/cm : 670 µs pulse was determined to be ~70% (**Figure 7A**). To highlight the importance of the system to accurately map out the degree of cell membrane permeabilization and select a sufficiently high electroporation pulse energy when transitioning to the high-throughput mode, the 0.4 kV/cm: 3 ms pulse condition was also explored in terms of eTE (**Figure 7B**). In this case, the resulting eTE at 24 hours was less than 5%.

[Place **Figure 7** Here]

FIGURE AND TABLE LEGENDS:

Figure 1: Experimental factors affecting electroporation outcomes. (Left) Cell Suspension—Important factors to consider prior to the onset of electroporation include: Payload (in this case, pDNA), concentration, cell density, and electroporation buffer properties. Electroporation buffer properties to consider are conductivity, osmolarity, and the exact molecular composition contributing to these values. (Middle) Pulse Application—The exact pulse-type (square wave vs. exponential decay) and pulse waveform (single pulse vs. pulse train) must be optimized to maximize both the resulting cell viability and electro-transfection efficiency. Common pulse trains implemented in electroporation processes are typically composed of a series of High Voltage (HV) pulses or series of pulses rotating between HV and Low Voltage (LV) pulse magnitudes. (Right) Cell Recovery—Down-stream processing steps, in particular, the recovery cell culture media that cells are transferred to, should be optimized. Not featured (Far Left), additional upstream cell processing steps can be implemented for overall electroporation process optimization.

Figure 2: Microdevice fabrication. (**A**) Microfluidic Channel Fabrication—Key Steps: Silicon Wafer

Cleaning (steps 2.1.1–2.1.3), Photoresist Coating and Soft Bake (steps 2.1.7–2.1.8), UV Exposure (step 2.1.10), Development (step 2.1.12), and PDMS Pouring (subsection 6.2). (**B**) Electrode Fabrication—Key Steps: Glass Slide Cleaning (steps 2.1.1–2.1.3), HMDS Coating and Photoresist Coating (steps 2.2.3–2.2.4), UV Exposure (step 2.2.8), Development (step 2.2.9), HF Etch (section 3), Physical Vapor Deposition (section 4), and Photoresist Lift-off (section 5). (**C**) Device Finalization—Key Steps: Inlet/Outlet Access and Sonication (step 6.2.3 and section 6.3), PDMS Bonding, and Wire Attachment (section 7).

Figure 3: Experimental setup schematic—Single cell detection. The high-power op-amp (PA-90) allows for the super-imposition of the high voltage electroporation pulse onto the lock-in Output AC signal that is required for the single-cell detection. This excitation signal passes through the micro-electroporation device (Device Under Test, DUT) where the current is then amplified by the current pre-amplifier and fed into the algorithm. The system continuously monitors for the cell detection event. Upon cell entry, a digital signal is generated by the lock-in amplifier to trigger the application of the electroporation pulse to the cell(s) in transit. Legend: PA-90 (high power op amp), DUT (device under test), DIO (digital input/output), FG—EP (function generator / electroporation pulse), 50X (50X amplifier), PS—V- (power supply / negative voltage for PA 90), FG—V+ (Function Generator, positive voltage for PA 90).

Figure 4: Single cell membrane permeabilization — Algorithm operation. (Top) Electrical recording of a series of single-cell detections / pulse applications (indicated by the sharp spikes in current). (Bottom) System operation for the detection and pulsing of a single cell. (1) System is continuously sensing for a change in the current, via a point-by-point slope calculation. (2) A sharp decrease in the slope is detected, indicative of the entry of a cell between the electrodes and triggers the computer-controlled pulse application. (3) A current drop (ΔI_C) is determined and is proportional to the size of the cell. (4) The electroporation pulse is applied to the cell in transit, causing a sensing artifact in the electrical signal (grey box). (5) The lock-in amplifier switches back to cell monitoring as it re-locks into the cell in transit. (6) The cell exits the electrode set, causing another, smaller magnitude spike in current ($\Delta I_C > (I_6 - I_5)$). The difference in the impedance measurements is due to pore formation through the insulated cell membrane. This change in current is termed the permeabilization current (ΔI_P). The degree of cell membrane permeabilization is calculated ($\Delta I_P/\Delta I_C$). The baseline stabilizes and the system returns to detection mode (1).

Figure 5: HEK293 cell membrane permeabilization mapping — $\Delta I_P / \Delta I_C$ versus electrical energy. The electrical data ($\Delta I_P / \Delta I_C$) is represented as the Mean ± SEM. Pulsing conditions (left to right)—0.4 kV/cm : 3 ms, 0.8 kV/cm : 1.5 ms, 1.0 kV/cm : 1.2 ms, 1.2 kV/cm : 1 ms, 1.8 kV/cm : 0.67 ms, 2.4 kV/cm : 0.5 ms. A clear correlation is observed between the degree of cell membrane permeabilization and the electrical energy density of the applied pulse. For this round of experimentation, the 1.8 kV/cm: 0.67 ms pulsing condition was selected as the 'optimal' electroporation pulse for the high-throughput module.

Figure 6: Cell-population-based feedback-controlled electroporation—Process workflow. To

start, an initial flow rate is programmed (Q_0) to allow for single-cell-level electrical interrogation. A programmable number of cells is pulsed at each pre-determined electroporation pulsing conditions (E_0/t_0 to E_N/t_N), with the applied electrical energy increasing with each iteration of electroporation pulse applications. Following the completion of the highest electrical energy pulse included in the study, E_N/t_N, the cell membrane permeabilization curve is plotted, and the optimal electroporation pulse is determined for the cell population under test. The system proceeds to high-throughput mode, where the flow rate is increased to $Q_{throughput,}$ and the rate-limiting single-cell interrogation steps are omitted. The optimal pulse train will be continuously applied E_{opt} / t_{opt} at $d.c._{opt}$ such that each cell in transit will receive a single electroporation pulse based on the cell transit time and the pulse width duty cycle (d.c.).

Figure 7: electro-Transfection Efficiency—GFP expression at 24 h. HEK293 cells were incubated at 37 °C for 24 hours following micro-electroporation experiments. All cells were stained with DRAQ5 (red), and the electro-transfection efficiency (eTE) was determined based on the ratio of cells expressing GFP (green) to the total cell number (red). Cell viability was not assessed as an outcome metric in this study. (**A**) Representative, stacked 4× fluorescence image of HEK293 cells successfully transfected via a 1.8 kV/cm: 670 µs pulse showing eTE of approximately 70%. (**B**) Representative, stacked 4× fluorescence image of HEK293 cells unsuccessfully transfected via a 0.4 kV/cm : 3 ms pulse showing eTE << 5%. Scale bar: 100 µm.

Table 1: Electroporation pulse parameters. For this study, electroporation pulses were chosen such that the charge flux ($\sigma \times E \times t$) remains constant, where σ is the solution conductivity (S/cm), E is the electric field strength (kV/cm) and t is the pulse duration (ms). The result is a spectrum of the applied pulse electrical energy. Examples of the required duty cycle (d.c.) to achieve the specified pulse parameters are provided for both a 5× and 10× increase in the initial (single-cell-detection) flow rate.

Supplementary Figure 1: 2-Dimensional CAD schematic. The micro-electroporation device consists of a straight, 100 µm wide micro-channel with a 1 mm diameter inlet and a 3 mm diameter outlet. Each electrode trace is 100 µm wide and the electrode set encompasses the electroporation region of the device, which is 300 µm long. The 3-dimensional height of the micro-channel is controlled by the thickness of the photoresist. In this work, the height of the device was 20 µm.

DISCUSSION:

The methodology presented within this protocol primarily focuses on the microfabrication of a microfluidic device that is then integrated into a specialized electroporation experimental setup. The term 'recipe', which is often used when describing the specifics of the microfabrication process, hints at the importance of following/optimizing each step to successfully fabricate a functioning device. However, certain critical steps within the process, when not optimized, such as UV exposure time/energy, PVD sputtering rates/durations, and oxygen plasma generator settings, can be problematic to both the fabrication process as well as the successful execution of the electroporation experiments. Troubleshooting the fabrication process is primarily done via trial and error or a more controlled Design of Experiments experimental design. Additionally,

there are alternative microfabrication techniques, such as Deep Reactive Ion Etching (DRIE), that can be substituted to perform the different steps within the protocol (i.e., using a DRIE etched molding structure to perform the soft lithography process). Furthermore, optimizing recipes and designing/fabricating devices can be time-consuming for novices in the field. However, once the microfabrication process has been successfully developed, the engineer/scientist has the freedom to design a device that is suitable to their specific needs.

To that end, the device described within this protocol was developed to expand upon our previous work[32]. This entailed the utilization of the single-cell membrane permeabilization electrical detection but in a higher-throughput manner. The experimental setup described within requires the need for specialized equipment, i.e., lock-in amplifier, that may be uncommon to the standard research lab and thus limiting the potential outreach and adaptability of this technique. However, a 'bare-bones' microfluidic electroporation device can be implemented following this protocol, requiring only a function generator and possibly a voltage amplifier to generate the electroporation pulses.

Nevertheless, this micro-electroporation platform distinguishes itself from other single-cell electroporation technologies. The ability to both electrically detect and optimize electroporation parameters on a single-cell suspension in a continuous-flow environment is truly innovative. Future work involves optimizing the other important experimental parameters related to successful electroporation outcomes (see **Figure** 1) to further improve the overall effectiveness of this platform. Additional viability and metabolic assays will be developed and implemented to assess any potential negative downstream effects associated with the micro-electroporation platform. Furthermore, the microfluidic design can continue to be improved upon to achieve higher cellular throughput, as has been demonstrated by other groups[40]. Upon addressing these concerns, this technology has the potential to be adopted into the cell therapy manufacturing process to perform gene delivery and/or gene editing, as this methodology is highly amenable to both a closed and automated process.

ACKNOWLEDGMENTS:
The authors would like to acknowledge financial support by the National Science Foundation (NSF CBET 0967598, DBI IDBR 1353918) and the U.S. Department of Education's Graduate Training in Emerging Areas of Precision and Personalized Medicine (P200A150131) for funding graduate student J.J.S. on fellowship.

DISCLOSURES:
The authors have nothing to disclose.

REFERENCES:
1 Gao, Q. Q. et al. Therapeutic potential of CRISPR/Cas9 gene editing in engineered T-cell therapy. *Cancer Medicine.* **8** (9), 4254–4264 (2019).
2 Aijaz, A. et al. Biomanufacturing for clinically advanced cell therapies. *Nature Biomedical Engineering.* **2** (6), 362–376 (2018).
3 Milone, M. C., O'Doherty, U. Clinical use of lentiviral vectors. *Leukemia.* **32** (7), 1529–1541

(2018).
4 Weaver, J. C., Chizmadzhev, Y. A. Theory of electroporation: A review. *Bioelectrochemistry and Bioenergetics.* **41** (2), 135–160 (1996).
5 Kotnik, T., Rems, L., Tarek, M., Miklavcic, D. Membrane electroporation and electropermeabilization: mechanisms and models. *Annual Review of Biophysics.* **48**, 63–91 (2019).
6 Rosazza, C., Meglic, S. H., Zumbusch, A., Rols, M. P., Miklavcic, D. Gene electrotransfer: A mechanistic perspective. *Current Gene Therapy.* **16** (2), 98–129 (2016).
7 Clauss, J. et al. Efficient non-viral T-cell engineering by sleeping beauty minicircles diminishing DNA toxicity and miRNAs silencing the endogenous T-cell receptors. *Human Gene Therapy.* **29** (5), 569–584 (2018).
8 Sherba, J. J. et al. The effects of electroporation buffer composition on cell viability and electro-transfection efficiency. *Scientific Reports.* **10** (1), 3053 (2020).
9 Lu, H., Schmidt, M. A., Jensen, K. F. A microfluidic electroporation device for cell lysis. *Lab on a Chip.* **5** (1), 23–29 (2005).
10 Kar, S. et al. Single-cell electroporation: current trends, applications and future prospects. *Journal of Micromechanics and Microengineering.* **28** (12), (2018).
11 Shi, J. F. et al. A review on electroporation-based intracellular delivery. *Molecules.* **23** (11), (2018).
12 Wang, S. N., Zhang, X. L., Wang, W. X., Lee, L. J. Semicontinuous flow electroporation chip for high-throughput transfection on mammalian cells. *Analytical Chemistry.* **81** (11), 4414–4421 (2009).
13 Wei, W. J. et al. An implantable microelectrode array for simultaneous L-glutamate and electrophysiological recordings in vivo. *Microsystems & Nanoengineering.* **1**, (2015).
14 Maschietto, M., Dal Maschio, M., Girardi, S., Vassanelli, S. In situ electroporation of mammalian cells through SiO2 thin film capacitive microelectrodes. *Scientific Reports.* **11** (1), (2021).
15 Wu, Q. R. et al. Organ-on-a-chip: recent breakthroughs and future prospects. *Biomedical Engineering Online.* **19** (1), (2020).
16 Pandey, C. M. et al. Microfluidics Based Point-of-Care Diagnostics. *Biotechnology Journal.* **13** (1), (2018).
17 Vigneshvar, S., Sudhakumari, C. C., Senthilkumaran, B., Prakash, H. Recent advances in biosensor technology for potential applications - An overview. *Frontiers in Bioengineering and Biotechnology.* **4**, (2016).
18 Nuxoll, E. BioMEMS in drug delivery. *Advanced Drug Delivery Reviews.* **65** (11–12), 1611–1625 (2013).
19 Kang, S., Kim, K. H., Kim, Y. C. A novel electroporation system for efficient molecular delivery into Chlamydomonas reinhardtii with a 3-dimensional microelectrode. *Scientific Reports.* **5**, (2015).
20 Zheng, M. D., Shan, J. W., Lin, H., Shreiber, D. I., Zahn, J. D. Hydrodynamically controlled cell rotation in an electroporation microchip to circumferentially deliver molecules into single cells. *Microfluidics and Nanofluidics.* **20** (1), (2016).
21 Santra, T. S., Kar, S., Chang, H. Y., Tseng, F. G. Nano-localized single-cell nano-electroporation. *Lab on a Chip.* **20** (22), 4194–4204 (2020).

22 Lee, W. G., Demirci, U., Khademhosseini, A. Microscale electroporation: challenges and perspectives for clinical applications. *Integrative Biology.* **1** (3), 242–251 (2009).
23 Santra, T. S., Chang, H. Y., Wang, P. C.,Tseng, F. G. Impact of pulse duration on localized single-cell nano-electroporation. *Analyst.* **139** (23), 6249–6258 (2014).
24 Geng, T., Lu, C. Microfluidic electroporation for cellular analysis and delivery. *Lab on a Chip.* **13** (19), 3803–3821 (2013).
25 Hsi, P. et al. Acoustophoretic rapid media exchange and continuous-flow electrotransfection of primary human T cells for applications in automated cellular therapy manufacturing. *Lab on a Chip.* **19** (18), 2978–2992 (2019).
26 Khine, M., Ionescu-Zanetti, C., Blatz, A., Wang, L. P., Lee, L. P. Single-cell electroporation arrays with real-time monitoring and feedback control. *Lab on a Chip.* **7** (4), 457–462 (2007).
27 Ye, Y. F. et al. Single-cell electroporation and real-time electrical monitoring on a microfluidic chip. *2020 33rd Ieee International Conference on Micro Electro Mechanical Systems (Mems 2020).* 1040–1043 (2020).
28 Huang, Y., Rubinsky, B. Microfabricated electroporation chip for single cell membrane permeabilization. *Sensors and Actuators a-Physical.* **89** (3), 242–249 (2001).
29 Guo, X. L., Zhu, R. Controllable in-situ cell electroporation with cell positioning and impedance monitoring using micro electrode array. *Scientific Reports.* **6**, (2016).
30 Punjiya, M., Nejad, H. R., Mathews, J., Levin, M., Sonkusale, S. A flow through device for simultaneous dielectrophoretic cell trapping and AC electroporation. *Scientific Reports.* **9**, (2019).
31 Wang, H. Y., Lu, C. Microfluidic electroporation for delivery of small molecules and genes into cells using a common DC power supply. *Biotechnology and Bioengineering.* **100** (3), 579–586 (2008).
32 Zheng, M. D. et al. Continuous-flow, electrically-triggered, single cell-level electroporation. *Technology.* **5** (1), 31–41 (2017).
33 Batista Napotnik, T., Miklavcic, D. In vitro electroporation detection methods - An overview. *Bioelectrochemistry.* **120**, 166–182 (2018).
34 KAYAKU. *MICROPOSIT™ S1800® G2 Series Photoresists*, <https://kayakuam.com/wp-content/uploads/2019/09/S1800-G2.pdf> (2021)
35 KAYAKU. *SU-8 2000 Permanent Negative Epoxy Photoresist*, <https://kayakuam.com/wp-content/uploads/2020/08/KAM-SU-8-2000-2000.5-2015-Datasheet-8.13.20-final.pdf> (2021)
36 MicroChemicals. *Substrate Preparation*, <https://www.microchemicals.com/technical_information/substrate_cleaning_adhesion_photoresist.pdf> (2021)
37 Lisinenkova, M., Hahn, L., Schulz, J. in *4M 2006 - Second International Conference on Multi-Material Micro Manufacture*. 91–94, Elsevier (2006).
38 Beh, C. W., Zhou, W. Z., Wang, T. H. PDMS-glass bonding using grafted polymeric adhesive - alternative process flow for compatibility with patterned biological molecules. *Lab on a Chip.* **12** (20), 4120–4127 (2012).
39 APEX. *PA90 High Voltage Power Operational Amplifiers*, <https://www.apexanalog.com/resources/products/pa90u.pdf> (2021)
40 Lissandrello, C. A. et al. High-throughput continuous-flow microfluidic electroporation of mRNA into primary human T cells for applications in cellular therapy manufacturing. *Scientific Reports.* **10** (1), 18045 (2020).

Figure1

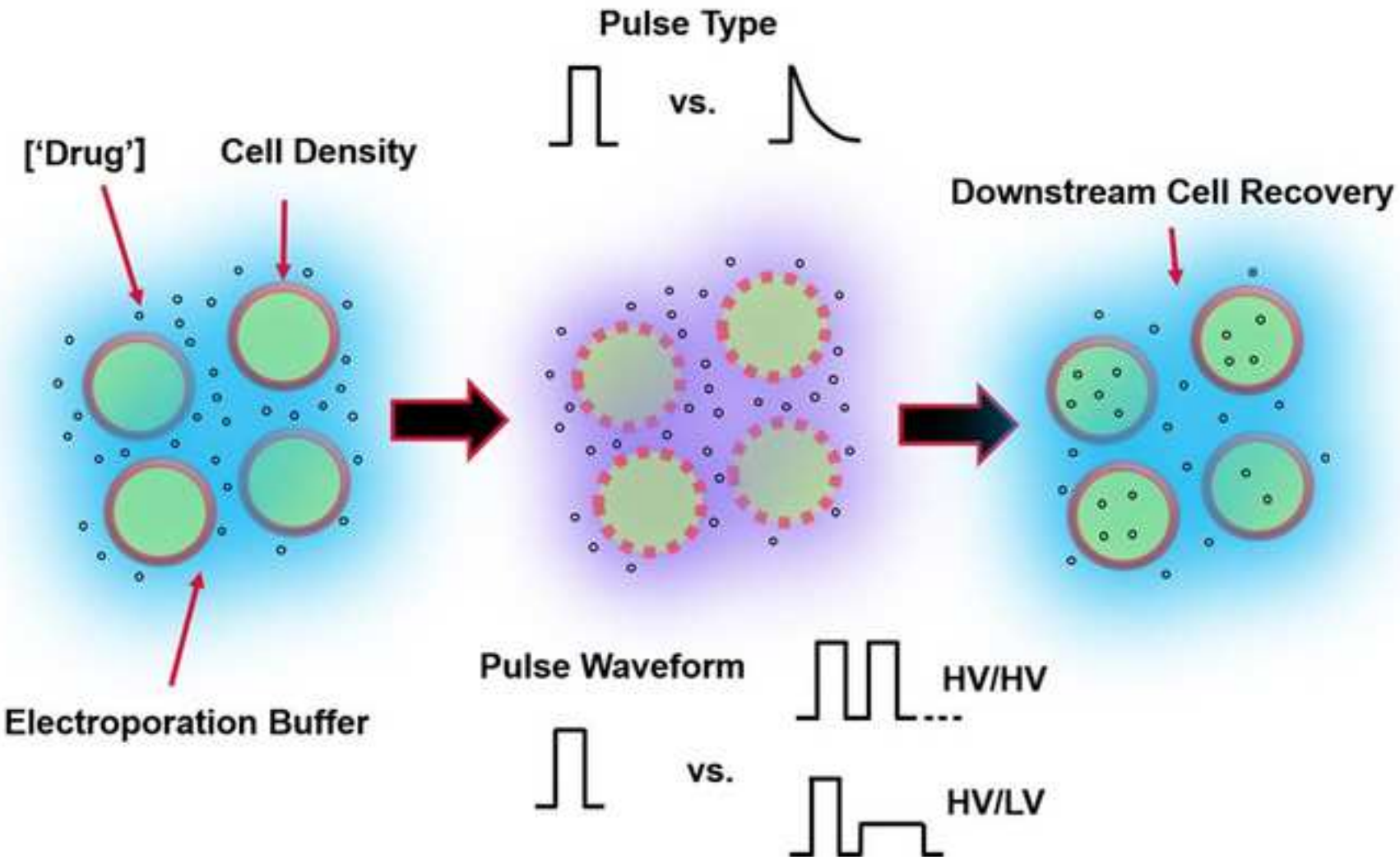

Figure 2

Click here to access/download;Figure;Updated Figure 2.png

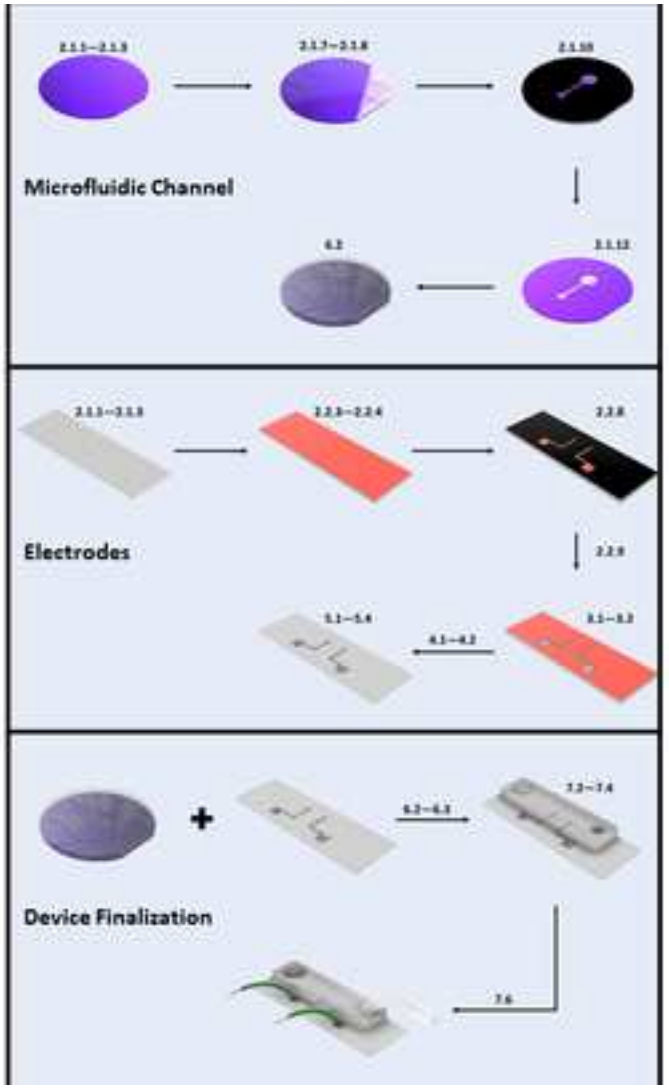

Figure 3

Click here to access/download;Figure;Figure3.jpg

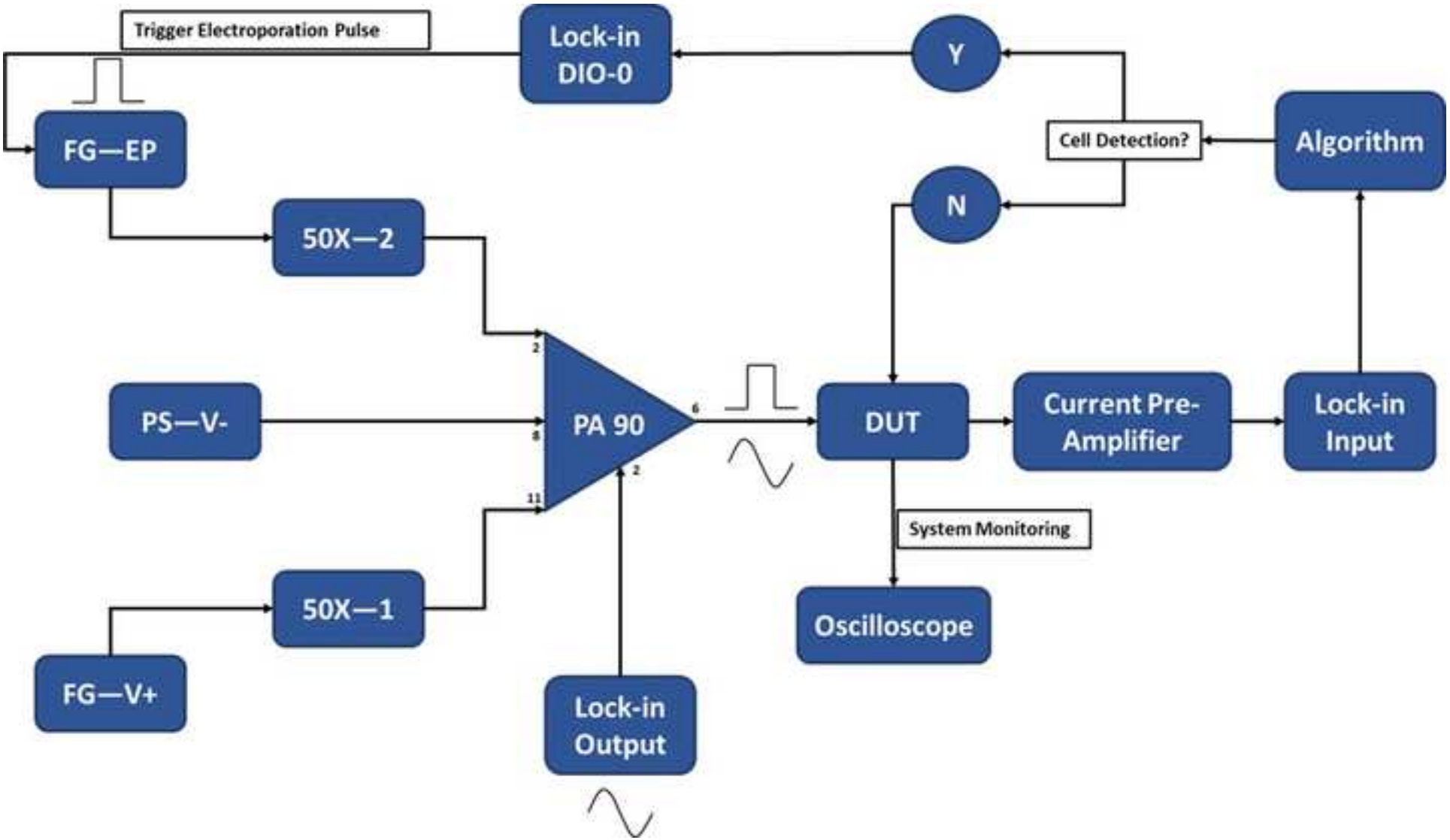

Figure 4

Click here to access/download;Figure;Figure4.jpg

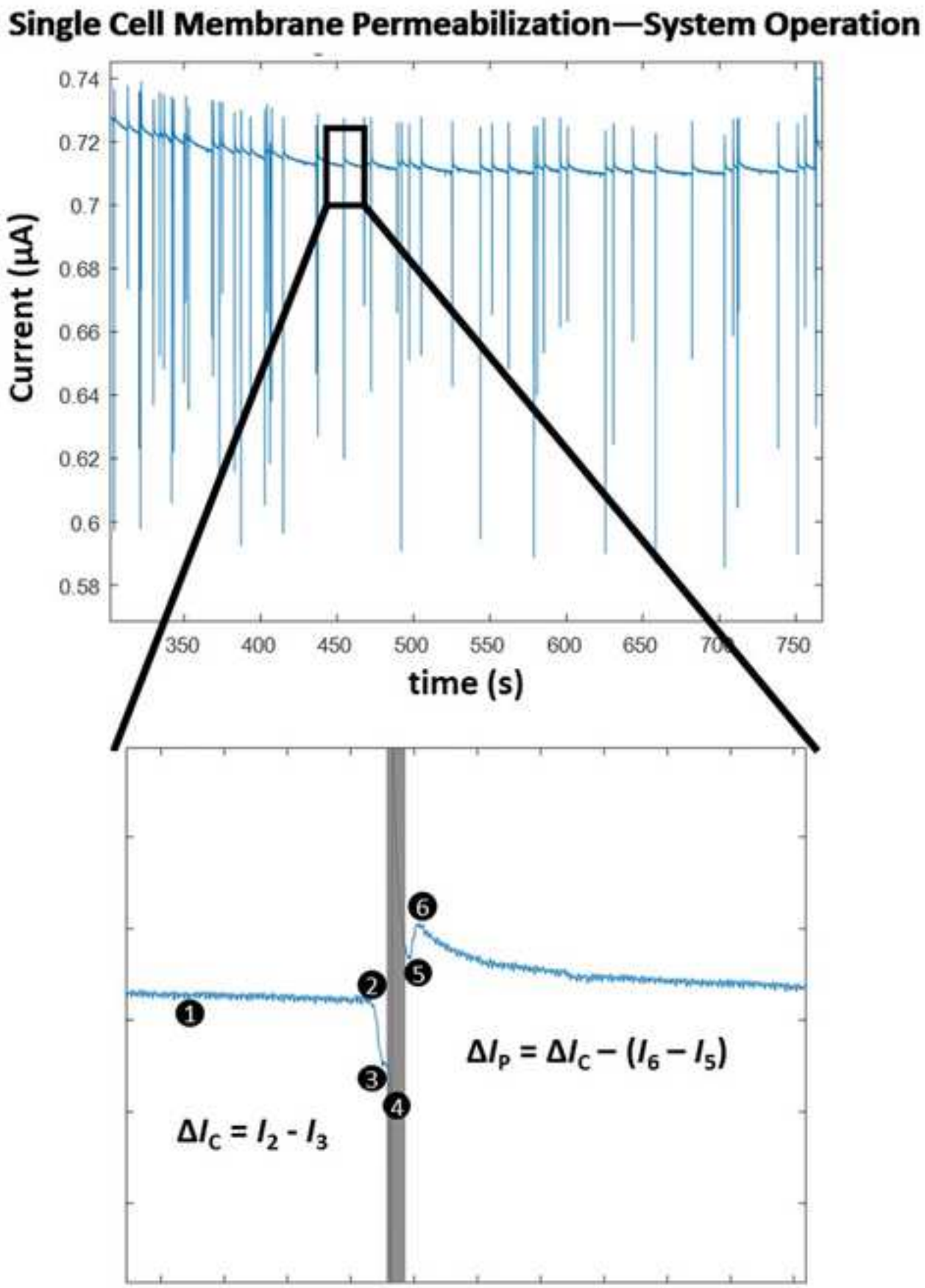

Figure 5

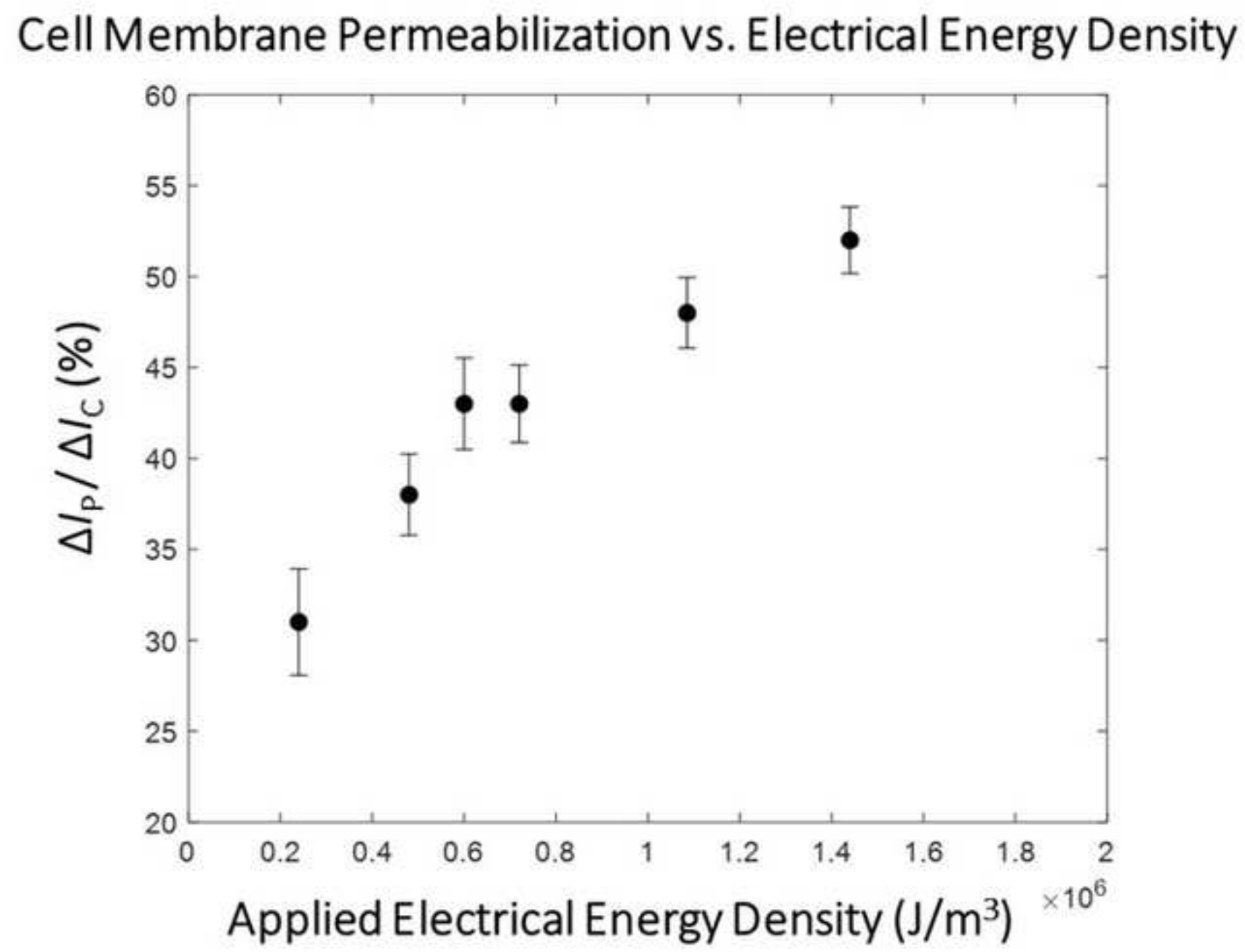

Figure 6

Click here to access/download;Figure;Figure6.jpg

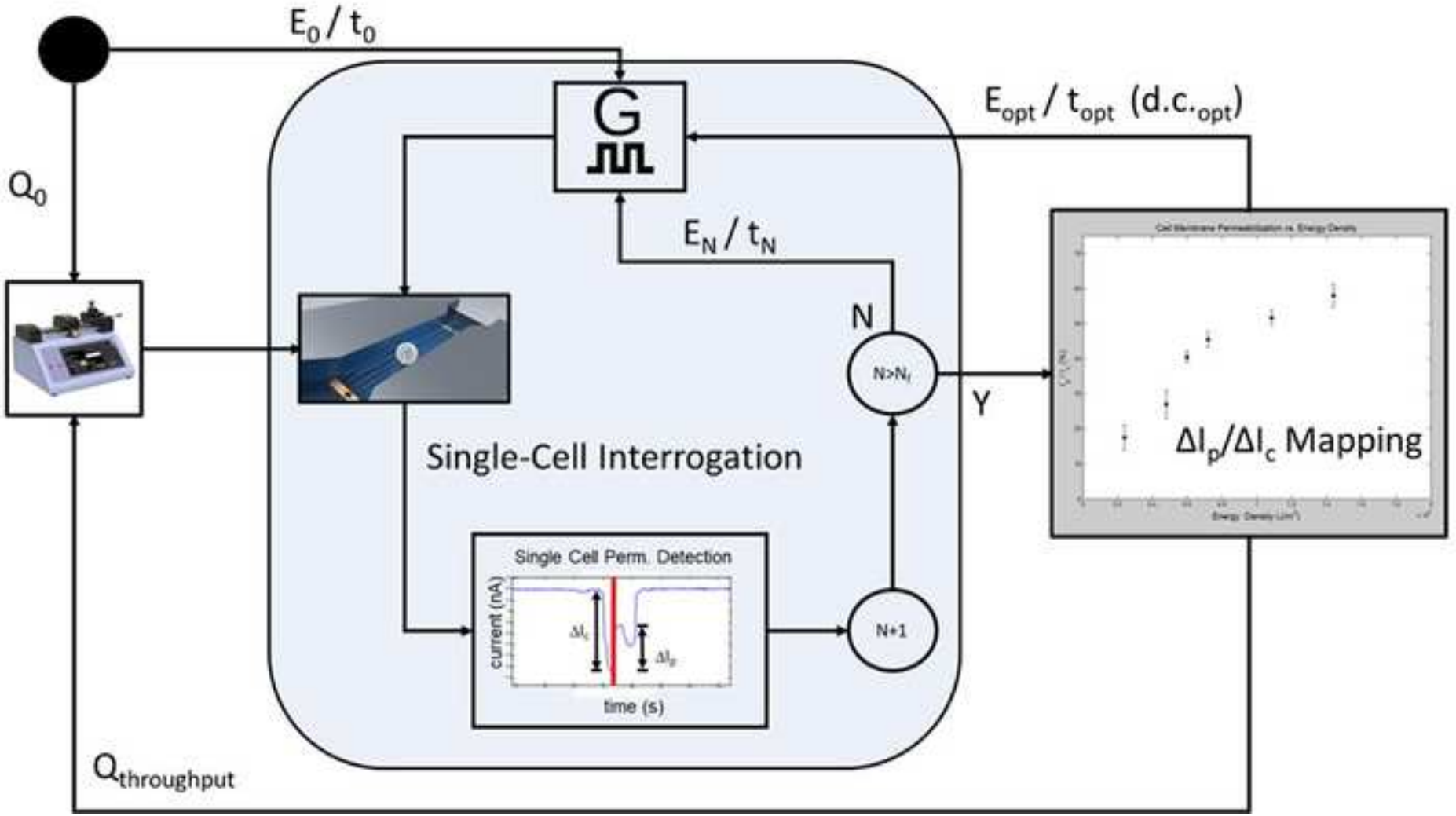

Figure 7

Click here to access/download;Figure;Figure7.JPG

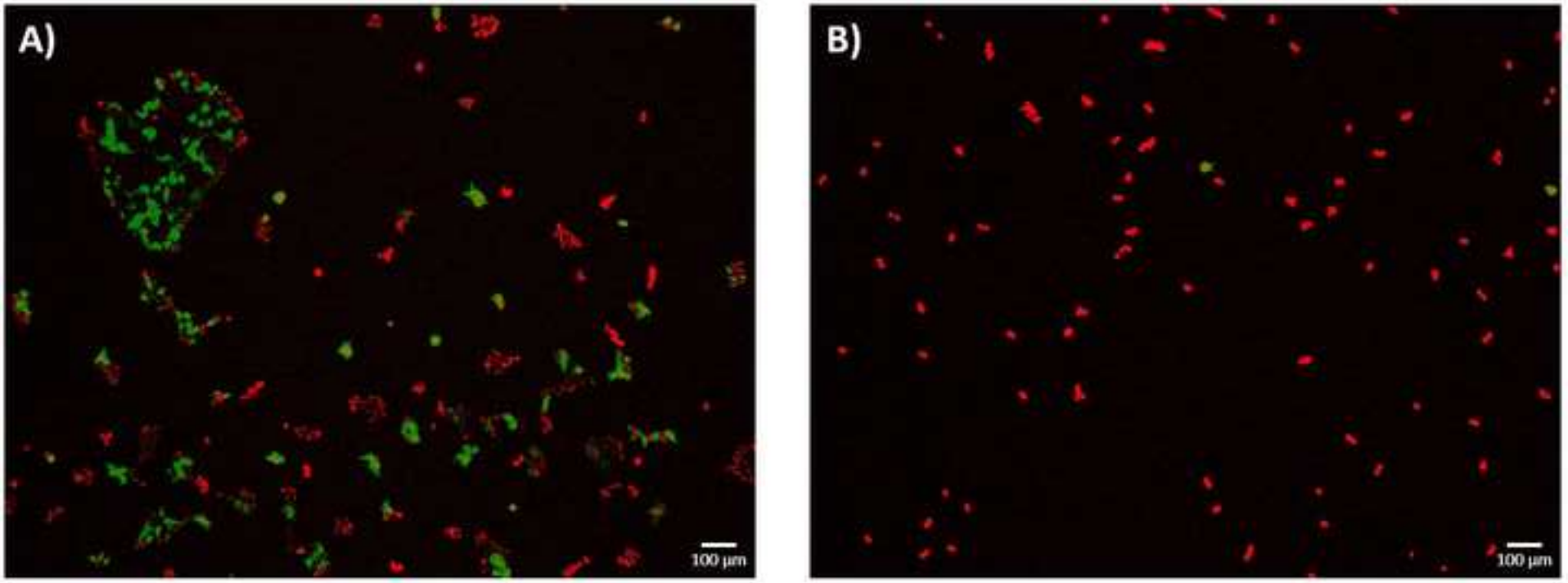

Table 1

	Single Cell Detection: (t_{trans} = 250 ms, d.c. = 100%)		High Throughput: (t_{trans} = 50 ms)	High Throughput: (t_{trans} = 25 ms)
	Electric Field Strength (kV/cm)	Pulse Duration (ms)	Duty Cycle (d.c.)	Duty Cycle (d.c.)
Increasing Pulse Electric Energy ↓	0.4	3.0	6.0	12
	0.8	1.5	3.0	6.0
	1.0	1.2	2.4	4.8
	1.2	1.0	2.0	4.0
	1.8	0.67	1.3	2.7
	2.4	0.5	1.0	2.0

RUTGERS

Jeffrey D. Zahn, Ph.D.
Professor
Department of Biomedical Engineering
Rutgers, The State University
599 Taylor Road
Piscataway, NJ 08854-5610

Email:jdzahn@soe.rutgers.edu
Phone:848-445-6587
Fax:732-445-3753

September 20, 2021

Prof. Xiaoyun Ding, Assistant Professor, University of Colorado Boulder.
Prof. Soojung Claire Hur, Assistant Professor, Johns Hopkins University.
Guest editors: *Journal of Visualized Experiments*

Dear Drs. Ding and Hur,

Please find attached a revision of the submitted manuscript JoVE63103 entitled "The Fabrication and Operation of a Micro-Electroporation System Capable of Both Membrane Permeabilization Detection and High Throughput Performance". This manuscript is being submitted for consideration for publication as a research article in the methods collection "Current methods for intracellular drug delivery and cell transfection" in the *Journal of Visualized Experiments (JoVE):*

As before, the focus of the manuscript is to describe the design, fabrication, and operation of a flow-through microfluidic electroporation platform capable of electrically-monitoring the degree of cell membrane permeabilization and determining optimal electroporation pulse settings for higher throughput transfection operation.

We would like to express our gratitude to the reviewers' constructive feedback and their recommendations for suggested revisions. The reviewers' careful review and thoughtful insights helped us provide more clarification to our fabrication details, clarify our protocol, expand our discussion of results, add additional references, and refine the manuscript in preparation for publication. The manuscript has also been lightly edited for readability and flow. In response to the reviewers' comments the manuscript been revised to address each of the reviewers' questions and concerns in detail. We feel that the revisions serve to make the manuscript stronger and of greater interest to JOVE's readership. The attached pages provide the specific responses to the reviewers' comments. In addition, a PDF version of this manuscript with showing the changes made is also attached.

We appreciate your further consideration of this original manuscript for publication in *Journal of Visualized Experiments*. This work is not being considered by any other journals.

If you have any questions feel free to contact me.

Sincerely,

Jeffrey D. Zahn, PhD

Editorial comments:

Changes to be made by the Author(s):

We thank the editor for taking the time to thoroughly review the manuscript and providing constructive feedback to improve the overall quality of this body of work. Please see below our responses to each of the line items and the corresponding changes made (when applicable).

1. Please take this opportunity to thoroughly proofread the manuscript to ensure that there are no spelling or grammar issues.

Thank you for providing the opportunity to perform additional proofreading the editing to the manuscript. Additional proofing of the manuscript was performed, and edits were implemented.

2. Please revise the following lines to avoid previously published work: 65-67, 649-650.

Thank you for pointing out the closeness of these sections to previously published material. Both lines 65-67 and 649-650 were re-written in the current draft of the manuscript.

65-67: "Electroporation,an alternative to viral-mediated gene delivery, relies on the application of an optimal electrical pulse waveform to perform DNA, RNA, and protein transfections of cells. Following the application of an external electric field , the cell membrane is briefly compromised, making the cell susceptible to the intracellular delivery of otherwise impermeable exogenous materials[4]."

649-650: "A distinct correlation is observed between the applied electrical energy and the degree of cell membrane permeabilization (**Figure 5**), with the existence of a transition region where a substantial increase in the degree of cell membrane permeabilization occurs."

3. JoVE cannot publish manuscripts containing commercial language. This includes trademark symbols (™), registered symbols (®), and company names before an instrument or reagent. Please remove all commercial language from your manuscript and use generic terms instead. All commercial products should be sufficiently referenced in the Table of Materials (including reagents, instruments, software, etc.). Please sort the Materials Table alphabetically by the name of the material.
For example, AutoCAD, EVG, Shipley, MicroPosit, MF, Stylus, MARCH, Apex Technologies, Zurich, Agilent, LabVIEW, etc.

Our apologies for the inclusion of commercial terminology. All references to these terms were removed from the body of the manuscript. Additionally, the materials table was sorted alphabetically by the name of the material

However, the example above is sorted by manufacturer. Let us know if you want to the sorted by the name of the manufacturer/company.

4. Please note that your protocol will be used to generate the script for the video and

must contain everything that you would like shown in the video. Please ensure you answer the "how" question, i.e., how is the step performed? Alternatively, add references to published material specifying how to perform the protocol action. There should be enough detail in each step to supplement the actions seen in the video so that viewers can easily replicate the protocol.

Thank you for the comment to ensure our protocol is 'user-friendly' to our end reader. Additional proofing and editing was performed to the protocol section to ensure clarity and readability for JoVE subscribers.

5. Please add more details to your protocol steps:
Line 182: Please provide a representation of the CAD design of the device with exact dimensions as a Supplementary document to help readers understand the device architecture.

A reference to 'Supplementary Figure 1' was provided in lines 196-197. A separate supplementary document with a CAD representation of our device will be uploaded upon resubmission.

Line 363: What is meant by surgically cut out?

Thank you for realizing the ambiguity of this wording. The use of the term 'surgically' was removed and replaced with the phrase 'Using the tip of a razor blade'

Line 421: Aspiration done with a pipette?

Sorry for the lack of detail. Additional information was added for clarity: "Aspirate media using either pipette or vacuum-system".

Line 449/452: Please convert centrifuge speeds to centrifugal force (x g) instead of revolutions per minute (rpm).

The centrifuge speed was converted from rpm to x g and was updated in all locations in the manuscripts.

Line 511: Any particular pressure to be applied?

Thank you for the comment. There is no exact amount of 'correct pressure' for this step. However, additional details were provided to help the reader better understand how to execute this step: "Using your thumb, gently apply pressure to the plunger such that the fluid slowly reaches the end of the tubing line."

6. In the software, please ensure that all button clicks and user inputs are provided throughout. Also, please ensure that the button clicks are bolded.

Thank you for the comment. The button clicks mentioned in the protocol were formatted 'bold' and all user inputs were previously referenced.

7. Please include all the Figure/Table Legends together at the end of the Representative Results in the manuscript text.

The figure/table legends were copy & pasted to the end of the representative results section in addition to being accompanied by the figure in the 'Figure/Tables' section.

8. Figure 3: Please remove all the commercial terms from the Figure representation.

Figure 3 was updated, substituting generic terms for the commercial terminology.

9. Figure 7: Please include scale bars.

Thank you for pointing out the need for scale bars on these images. The images were updated to include the scale bars.

10. As we are a methods journal, please revise the Discussion to explicitly cover the following in detail in 3-6 paragraphs with citations:
a) Critical steps within the protocol

The paragraph speaking to the critical fabrication steps was re-phrased to explicitly state the term 'critical' :

"However, certain critical steps within the process, when not optimized, such as UV exposure time/energy, PVD sputtering rates/durations, and oxygen plasma generator settings, can be problematic to both the fabrication process as well as the successful execution of the electroporation experiments."

b) Any modifications and troubleshooting of the technique

The troubleshooting process for the microfabrication steps was explicitly stated and a line stating the availability of alternative methodology or modifications to the protocol was added including Deep Reactive Ion Etching as suggested by Reviewer #1:

"Troubleshooting the fabrication process is primarily done via trial and error or a more controlled Design of Experiments experimental design. Additionally, there are alternative microfabrication techniques, such as Deep Reactive Ion Etching (DRIE), that can be substituted to perform the different steps within the protocol (i.e., soft lithography in the case of DRIE)."

c) Any limitations of the technique

The limitations of the technique were further explained in the discussion:

”The experimental setup described within requires the need for specialized equipment, i.e., lock-in amplifier, that may be uncommon to the standard research lab and thus limiting the potential outreach and adaptability of this technique.”

d) The significance with respect to existing methods

The significance with respect to existing methods is touched on in the 3rd paragraph of the discussion:

“Nevertheless, this micro-electroporation platform distinguishes itself from other single-cell electroporation technologies. The ability to both electrically detect and optimize electroporation parameters on a single-cell suspension, in a continuous-flow environment is truly innovative.”

e) Any future applications of the techniques

Future applications were further touched upon in the final paragraph of the discussion

“Future work involves the optimization of the other important experimental parameters related to successful electroporation outcomes (See **Figure** 1) to further improve on the overall effectiveness of this platform. Additional viability and metabolic assays will be developed and implemented to assess any potential negative downstream effects associated with the micro-electroporation platform. Furthermore, the microfluidic design can continue to be improved upon to achieve a higher cellular throughput as has been demonstrated by other groups[35]. Upon addressing these concerns, this technology has the potential to be adopted into the cell therapy manufacturing process to perform gene delivery and/or gene editing, as this methodology is highly amenable to both a closed and automated process.”

Reviewers' comments:

Reviewer #1:

Manuscript Summary:

This protocol describes the standard microfabrication, experimental setup, and operation procedure of microfluidic electroporation, which attracts more and more attentions due to it advantages over bulk electroporation. GFP DNA plasmid and HEK293 cells are used in this protocol as demonstration. The real time monitoring of cell membrane permeabilization further increases the novelty and value of this work. It should be accepted to JoVE asap.

We thank the reviewer for taking the time to thoroughly review the manuscript and for the suggestion to be accepted into the journal.

Major Concerns:

NA

Minor Concerns:

A minor comment: in protocol 1.2.1., PDMS channel mold is based on SU8 photoresist, I will suggest adding a few sentences to discuss another option to make PDMS mold, the silicon mold made by DRIE etching. This does not need to be demonstrated in the followed video, but at least shows another common alternative approach to make the mold.

Thank you for the suggestion of adding details surrounding alternative approaches to perform the microfabrication steps. To address this comment, additional information was included in the discussion in relation to the troubleshooting and modifications of the protocol:

“Troubleshooting the fabrication process is primarily done via trial and error or a more controlled Design of Experiments experimental design. Additionally, there are alternative microfabrication techniques, such as Deep Reactive Ion Etching (DRIE), that can be substituted to perform the different steps within the protocol (i.e., soft lithography in the case of DRIE).”

Reviewer #2:

Manuscript Summary:

Sherba et al demonstrated continuous flow based electroporation technique, where they used cell-population-based feedback control for cell permeabilization and response to a variety of electroporation pulsing conditions, and determines the best electroporation pulse conditions for the cell type under test. The author successfully delivered DNA plasmid into HEK293 cells. The overall manuscript is interesting and written well. However there are a couple of grammatical mistake throughout this manuscript and author need to revise this manuscript for final acceptance.

We thank the reviewer for their comments and for taking the time to thoroughly read and review the manuscript. The authors have used this opportunity to perform additional proofreading and editing of the manuscript.

Major Concerns:

the author demonstrated the plasmid delivery efficiency, but they are not provided the viability data. This is important to provide the viability data for different days. In many electroporation cases, protein can express into cells after 24 hours, but most of the cells can be dead. Thus it is necessary at least to provide some dye staining viability data for different days to show the usefulness of this device.

The authors agree that the inclusion of viability data is of high importance. The main focus of this manuscript was the fabrication of the micro-electroporation device such that others in the field could adapt to their needs / equipment available. The inclusion of the GFP electro-transfection was to show a potential use of the experimental setup described within the manuscript. However, to speak to the need of the viability / metabolic assay post electroporation, additional information was provided in the discussion as necessary future work:

“Additional viability and metabolic assays will be developed and implemented to assess any potential negative downstream effects associated with the micro-electroporation platform.”

Minor Concerns:

In introduction part, author discuss the importance of microfabrication based single-cell microelectroporation process. But in recent year single-cell nanoelectroporation (Lab on a chip, 2020, IEEE Nanotechnology Magazine 2014 and many more) concept came and author need to revise the introduction part and need to provide the importance of single-cell nanoelectroporation with recent references. Moreover there are couple of high throughput single-cell electroporation devices has been reported (including patent). Author need to include these references.

Thank you for providing insight into the need to mention nano-EP. We have updated the Intro to include this mentioning. Additionally, the following references were added where appropriate to the introduction:

Santra, T. S., Kar, S., Chang, H. Y. & Tseng, F. G. Nano-localized single-cell nano-electroporation. *Lab on a Chip.* **20** (22), 4194-4204, (2020).

Santra, T. S., Chang, H. Y., Wang, P. C. & Tseng, F. G. Impact of pulse duration on localized single-cell nano-electroporation. *Analyst.* **139** (23), 6249-6258, (2014).

Ye, Y. F. *et al.* Single-Cell Electroporation and Real-Time Electrical Monitoring on a Microfluidic Chip. *2020 33rd Ieee International Conference on Micro Electro Mechanical Systems (Mems 2020).* 1040-1043, (2020).

Punjiya, M., Nejad, H. R., Mathews, J., Levin, M. & Sonkusale, S. A flow through device for simultaneous dielectrophoretic cell trapping and AC electroporation. *Scientific Reports.* **9**, (2019).

Few minor comments:
Line 242-need to mention exact post bake temperature

The temperature is mentioned in the text: “Place the SU-8 coated silicon wafer on a hot plate at 95 °C for 4—5 minutes for post exposure bake.”

Also, the reader is warned at the start of the procedure that these exact steps will need to be optimized in their cleanroom setting.

Line-245- need to mention exact development time.

The development time is mentioned in the text: “Submerge the silicon wafer in the SU-8 developer solution for 3—4 minutes. Apply gentle agitation. Remove wafer from solution and rinse surface with IPA.”

Also, the reader is warned at the start of the procedure that these exact steps will need to be optimized in their cleanroom setting.

Line 269-need to do the sentence correction "approximately of approximately"

Thank you for pointing out this typo. The typo was fixed.

Reviewer #3:

Manuscript Summary:

The manuscript describes the design and preparation of a microfluidic device capable of applying electroporation pulses to single cell suspensions and measuring the degree of cell membrane permeabilization. The desgin of the microfluidic chamber is very detailed and reproducible. The description of the hardware is more difficult to follow appreciating that it is way more difficult to break it down in individual steps and components. Overall the manuscript is worth publishing as it will find interest in the biomedical community after the minor concerns listed below have been addressed.

The authors thank Reviewer 3 for taking the time to read through the manuscript and provide their feedback as well as their recommendation to publish this work in JoVE.

Minor Concerns:

Overall procedure: It should be emphasized more strongly in the text that pulse application is triggered by an individual cell passing across the first electrode - at least that is my understanding on the mechanism on how cell flow and electroporation pulse are synchronized such that the pulse is always delivered to the cells between the electrodes.

Thank you for providing your concerns on the overall clarity regarding one of the fundamental mechanisms for how the single-cell portion of the device operates. Clarity was provided in the procedure:

4.2.2: “Start the LabVIEW computer program by clicking ‘Run’ . Ensure the system is saving the electrical data. Ensure the system is reliably detecting cells to trigger the computer controlled pulse applications.”

Additional clarity was provided in both the results section and the figure caption:

“…there is an instantaneous increase in impedance, resulting in a sharp, decrease in the measured current, allowing for consistent cell detection (2), which ultimately triggers the computer controlled pulse application (4).”

“…(2) A sharp decrease in the slope is detected, indicative of the entry of a cell between the electrodes and triggers the pulse application”

The system automatically detects cell peremabilization. As figure 5 indicates, the permeabilization saturates with increasing energy density. This is highly anticipated. But electroporation is always a trade-off between loading efficiency and invasiveness. Neither one of them is determined online but only 24 h later by staining and microscopic inspection. Using a sufficiently high energy density may open the membranes irreversibly and the user will only know about this 24 h later. So to my standards, the part of the experiments that determines the electroporation parameters should be separated by the high throughput phase by 24 h to have access to the correlation between energy density and survival / loading efficiency. I would like to encourage the authors for a critical discussion to make sure the readers are aware of this. The authors have started a short discussion on this without expressing it in plain words. Please include this aspect in the discussion (very end) where the authors elaborate on the innovative combination

of applying electroporation pulses and measure the permeabilization of the cells at the same time.

Please include in situ electroporation in the introduction. This variant of electroporation has also been used to design micro-electroporation devices and should be mentioned to give the full picture.

Reference to in situ electroporation was included in the introduction:

"These advancements include the development of micro-electrode arrays for *in vivo* electrical monitoring[13], capacitive micro-electrodes for in situ electroporation[14],…"

Maschietto, M., Dal Maschio, M., Girardi, S. & Vassanelli, S. In situ electroporation of mammalian cells through SiO2 thin film capacitive microelectrodes. *Scientific Reports.* **11** (1), (2021).

2.1.1.2 Please provide concentration of trypsin. There are two different concentrations commercially available.

Thank you for pointing out this discrepancy. The concentration (0.25% trypsin-EDTA) was added to section 2.1.1.2 of the manuscript.

2.1.1.2 Please provide the centrifugal acceleration in units of g insteand of rpm to make it independent of centrifuge.

Thank you for the comment to make the centrifugation speeds more universally acceptable. The 2000 rpm was converted to the appropriate centrifuge 770 x g speed throughout the manuscript.

2.2.1 Obviously the device requires a specific electroporation buffer without the physiological concentrations of ions. This should be stated in the introduction as there are other devices available that can operate with physiological medium. Moreover, the authors should give pH and osmolality of the receipe described in 2.2.1.

This is a good point regarding the conductivity, as the lower conductivity buffer was required to ensure sensitivity for some of the electrical measurements. A statement regarding this was added to the intro:

"Through the use of a hypo-physiologic conductivity electroporation buffer, this system allows for the electrical interrogation of single cells across a multitude of electroporation pulse applications"

Additionally, the pH and osmolality were added to section 2.2.1 "285 mM Sucrose, 0.7 mM MgCl2, 1mM KCl, 10 mM HEPES, 3mM NaOH (pH: 7.4; osmolality: 310 mOsm, conductivity: 500 µS/cm).".

2.3.1 Give centrifuge acceleration in units of g.

See previous comment.

2.3.2 Why is the range of cell number per mL so big ? Isn't there an optimum cell density ?

To ensure no discrepancies, this cell number was set to 5 million cells / mL. Additionally a note was adding stating the fact that the density will need to be optimized per cell type under study:

“Resuspend cells in electroporation buffer at approximately 5 million cells/mL. NOTE: Cell density should be optimized per cell type.”

3.2.2 Please use proper terminology here and along entire manuscript: pulse amplitude (in V) instead of pulse strength.

Thank you for pointing out the interchangeable use of ‘strength’ when the correct terminology would be ‘amplitude’. The manuscript was changed where appropriate to say pulse amplitude, when referring to the voltage of the pulse. However, when referring to the electric field strength the units are typically reported in ‘kV/cm’ in the electroporation literature. This was left untouched.

Section 3 is not easy to follow. The descriptions in the text are difficult to relate to figure 3. Please use the same terms in the text and in the figure. The descriptions were not entirely clear to the reviewer. I seriously doubt that the protocoll as it is right now is easily reproduced by the readership of J. Vis. Exp.

Thank you for pointing out the difficulty in following this section. Some additional terminology was implemented to further match up the protocol text / corresponding figure.

4.1.6 It seems that the second sentence of this section should should have been mentioned earlier.

Thank you for pointing out this confusion. This text was moved to section 4.1.1.

Also the ‘pre-fill’ was changed to ‘re-fill’ for section 4.1.6.

Figure 4: Why is the current higher at time point 6 compared to the situation when the cell has left the space between electrodes ? Why is the current higher after the cell has left compared to the current before the cell has entered the space between the electrodes ? Why does the current fall when the electrooprated cell leaves the inter-electrode space. The reviewer would have expected it to rise back to the background level but not to fall. Even if the cell is partially permeabilized the current of the empty channel should be higher. Conductivity cannot be higher with the permeabilized cell in the sensitive volumne compare to no cell in the sensitive volume. Please include proper explanation.

Thank you for the comment. The first section of the ‘Representative Results’ was updated to clarify::

"**Figure 4** highlights the operation principles behind the single-cell-level membrane permeabilization detection for a single pulse amplitude. Following the initiation of the electroporation experiment, the cell detection algorithm determines an optimal threshold for cell detection via a point-by-point, slope-based detection method. The system then continuously monitors (1) for a significant negative change in the measured electrical current, which is indicative of the entry of a cell. This is due to the insulative nature of the biological cell membrane, such that when the cell traverses through the electrode set, there is an instantaneous increase in impedance, resulting in a sharp, decrease in the measured current, allowing for consistent cell detection (2), which ultimately triggers the switch to the computer-controlled pulse application (4). The insulated cell displaces a volume of electrolyte between the electrodes, resulting in a drop in current that is proportional to the size of the cell. This change in current is denoted as ΔI_C (3). Immediately following ΔI_C calculation, the pre-determined, electrical pulse is administered (4) to the cell in transit. This instantaneous influx of energy introduces a brief sensing artifact into the system (grey box). Upon re-locking onto the signal, i.e. switching back to cell monitoring, (5) it is evident that the electroporation pulse permeabilized the cell membrane as the magnitude of current change due to the cell's presence between the electrode set drops upon exit (6). The difference in the two drops in current due to the cell's impedance magnitude pre / post electroporation pulse application is termed the permeabilization current and is denoted as ΔI_P. Once the cell exits the volume between the electrodes, the baseline stabilizes, and the system returns back to cell detection mode (1)."

Additionally, the figure 4 caption was also adjusted accordingly:

"**Figure 4. Single Cell Membrane Permeabilization — Algorithm Operation.** (Top) Electrical recording of a series of single-cell detections / pulse applications (indicated by the sharp spikes in current). (Bottom) System operation for the detection and pulsing of a single cell. (1) System is continuously sensing for a change in the current, via a point-by-point slope calculation. (2) A sharp decrease in the slope is detected, indicative of the entry of a cell between the electrodes and triggers the computer-controlled pulse application. (3) A current drop (ΔI_C) is determined and is proportional to the size of the cell. (4) The electroporation pulse is applied to the cell in transit, causing a sensing artifact in the electrical signal (grey box). (5) The lock-in amplifier switches back to cell monitoring as it re-locks into the cell in transit. (6) The cell exits the electrode set, causing another, smaller magnitude spike in current ($\Delta I_C > (I_6 - I_5)$). The difference in the impedance measurements is due to pore formation through the insulated cell membrane. This change in current is termed the permeabilization current (ΔI_P). The degree of cell membrane permeabilization is calculated ($\Delta I_P/\Delta I_C$). The baseline stabilizes and the system returns to detection mode (1)."

Also: Regarding the calculation of the applied electrical energy: Did the authors use the conductivity of the pure buffer (please give the value) or the total conductivity in presence of a cell in between the electrodes for the calculation ? The latter seems to be more appropriate to get the proper energy with that equation since the cell is inside the inter-electrode volume during pulse application.

The conductivity of the electroporation buffer solution was added in section 2.2.1. Regarding the question about what conductivity was used in the calculation, this was stated in the 'Representative Results' section:

"Once each pre-determined electroporation pulse is tested, the $\Delta I_P / \Delta I_C$ is plotted against the applied electrical energy density ($\sigma \times E^2 \times t$), where σ is the solution conductivity (S/cm), E is the electric field strength (kV/cm), and t is the pulse duration (ms)."

Since the volume fraction of a cell in the electroporation region of the microfluidic device is negligible, we felt that it was acceptable to not include it for this calculation.

> For a 10 um diameter cell in our 100 um x 300 um x 20 um channel, the volume fraction of the single cell is << 1% of the total volume between the electrodes.

For the eTE: Shouldn't the transfected cells show a yellow emission (overlay of red and green) ? The cells seem either red or green but not yellow. Maybe this is due to the individual settings for the green and red channel. Please explain and advise.

For the imaging, 2 separate images were taken at the exact same location (Red and Green channels on the fluorescent microscope). These two images were then stacked on top of each other in imageJ, such that the Red and Green were separate entities.

Materials Tables: Please use separation lines to make the table more readable and avoid misalignment.

Separation lines have been added to the table. All fields appear as single lines on our copy of Microsoft excel but may display different on different computers depending on their software version and settings.

Supplementary Figure 1

Click here to access/download;Supplemental File (Figures, Permissions, etc.);Supplementary File 1-R2.pdf